

## **Interannual Variability of Summer Surface Mass Balance and Surface Melting in the Amundsen Sector, West Antarctica**

Marion Donat-Magnin<sup>1</sup>, Nicolas C. Jourdain<sup>1</sup>, Hubert Gallée<sup>1</sup>, Charles Amory<sup>3</sup>, Christoph Kittel<sup>3</sup>, Xavier Fettweis<sup>3</sup>, Jonathan D. Wille<sup>1</sup>, Vincent Favier<sup>1</sup>, Amine Drira<sup>1</sup>, Cécile Agosta<sup>2</sup>

---

### **Interactive comment by Reviewer #1**

Summary – The authors present a significant amount of work on MAR model validation and ultimate evaluation of drives of summer surface mass balance (SMB) and melt over the Amundsen Sea sector of Antarctica. They provide ample background of previous studies of the climate in West Antarctica, MAR model description as well as numerous observations used in the evaluation, full descriptions of the climate indices investigated, and, of course, their findings. The model reproduced temperature, wind speed, SMB, and melt intensity and days, and thus, the authors indicate that MAR is sufficient to evaluate drivers of SMB and melt in this sector. Specifically, they find that the longitudinal position of the Amundsen Sea Low (ASL) is the primary driver (relative to ENSO and the Southern Annular Mode, SAM) of SMB variability, whereas the variability in the ASL central pressure and to a lesser extent ENSO drive melt with increasing control moving westward. The SAM was not strongly related to either SMB or melt. The authors finally surmise that there might be a 6-month lag between ENSO and West Antarctic climate via either sea ice anomalies and their transport or a lag in Circumpolar Deep Water intrusions.

The paper is generally well written and very thorough (much appreciated!) and is organized in a logical fashion. Many of the insights are not necessarily new; however, the paper presents new model work and output and attempts to present a cohesive picture of drivers of West Antarctic climate. All of the analyses presented appeared appropriate and well thought out, and the tools used were appropriate. The work presented is very thorough yet easy to understand, making it a pleasure to read.

[We thank Reviewer #1 for this constructive and motivating feedback. We agree with most of the following objections and have considered them in the revised manuscript.](#)

### **Major Comments :**

One important consideration that is missing is a description of why summer SMB is critical and how it relates to the annual SMB. December-January-February (DJF) clearly are the relevant months for surface melting, but I think there should be more discussion as to why the paper specific isolated summer SMB. Specifically, melt is the highest in DJF, but snowfall is typically the lowest in DJF (Lenaerts et al., 2012). Please consider evaluation of winter (or other seasons of SMB relevance) or add language justifying the importance of summer SMB.

First of all, we would like to remind that annual SMB and surface melt rates (not only summer) are evaluated with respect to observations (Fig.4 and Fig.6). Then, we focus on a single season (summer) to analyze the teleconnections and associated mechanisms because the modes of variability and their teleconnections to the Amundsen Sea region both have strong seasonal characteristics, so that each season needs to be considered separately. We thought that analyzing all seasons separately would make the paper way too long, while showing the similarities and differences between the melt and SMB summer teleconnections was interesting. We agree that summer SMB is weaker than in other seasons, but it still represents 15% of the annual SMB (over the Amundsen Sea drainage basins) which is not negligible (vs 31%, 28% and 25% for MAM, JJA and SON respectively). The seasonal predictability of summer SMB from climate mode such as ENSO can also be of interest for operational prediction and summer field work. We have nonetheless included a supplementary table providing the correlation between SMB, and SAM, ENSO, ASL for other seasons (Table S3). The justification for the summer focus has also been added to the manuscript (section 1, L.130-134).

The relationship between melt and SMB is not investigated. The paper provides background on the importance of the role of melt on hydrofracture of ice shelves and potential rapid disintegration of an ice shelf, but it does not discuss the role of firn pore space. According to Table 2, nearly all of the surface melt refreezes within the firn column, so this mechanism should be introduced as well. The paper also notes that into the future there will be more snowfall and melt, but did not mention that the enhanced snowfall could potentially also provide more pore space for meltwater infiltration and refreezing. Please consider additional discussion of the role of SMB (or snowfall) on providing additional pore space for surface melt.

First, we apologize for a mistake : we omitted to mask nunataks in the basin averages, which slightly modified the values in table 2 (now updated).

For all drainage basins the runoff is indeed equal to zero, meaning that the firn is never saturated with melt water (which is a prerequisite to form runoff in our version of MAR). The minimum rate of surface melting + rainfall needed to saturate the annual snow layer (i.e. depleting all the air in the annual snow layer) can be estimated as  $snowfall * [p_{water}/p_{snow}] * [1 - p_{snow}/p_{ice}]$ , where snowfall is annual (in water equivalent), and  $\rho$  is the density of water snow and ice. Considering a fresh snow density of  $300 \text{ kg.m}^{-3}$  and ice density of  $920 \text{ kg.m}^{-3}$ , this means that the sum of annual melt and rainfall rates would need to exceed 2.25 times the annual snowfall value (all being expressed in water equivalent) to saturate the annual snow layer. This does not occur in any of the drainage basins in any year, indicating that meltwater ponding and complex surface hydrological flows are unlikely to develop over the West Antarctic drainage basins with such amount of precipitation and surface melting. The rate of surface water production (rainfall + melting) would need to increase by nearly two orders of magnitude to saturate present-day annual snow layer and therefore to initiate hydrofracturing. This is possible for strong warming scenarios given the exponential temperature dependence described by Trusel et al. (2015), although snowfall is also expected to increase (Krinner et al. 2008; Agosta et al., 2013; Ligtenberg et al., 2013; Lenaerts et al., 2016; Palerme et al., 2017), requiring even more meltwater to reach saturation.

This discussion has been added to section 4, L.634-642 and L.692-697.

There is no discussion on the relatively small proportions of variance explained by the climate indices. For instance, over western WAIS 20-40% of the summer SMB variability can be explained by the ASL longitude; however, it explains <6% of the Abbot, Cosgrove, and Pine Island catchments. None of the indices is significantly correlated with SMB over those catchments. Thus, the impact of ASL longitude is only relevant from Thwaites moving westward. The paper should make this clear and also potentially investigate other drivers of change for the eastern catchments or at least add clarifying statements that the drivers in eastern WAIS are unknown and potentially postulate why. Along similar lines, while ASL central pressure is a clear control on all catchments, the explained variance range from 12-21%, suggesting that there are additional factors at play when it comes to surface melt. Would investigation of multiple regression with the different indices help clarify how they interplay (for example, perhaps the combination of some movement and strengthening or weakening of the ASL is more strongly related). Please consider adding more multivariate relationships and discuss other potential influences on meltwater production since only a small portion is explained.

First of all, we have replaced NINO34 with (-SOI) throughout our paper because, as indicated by Holland et al. (2019), SOI gives slightly stronger correlations than NINO34.

Following the Reviewer's suggestion, we have investigated multi-linear regression (using a least shrinkage and selection operator (LASSO, Tibshirani 1996)) of summer SMB and melt rates onto the non-dimensionalized climate indices (divided by their standard deviation). The variance explained by individual regression coefficients are very close to the ones obtained by simple correlation, but considering the entire regression clearly shows that we are able to explain a larger portion of the SMB and melt rate variance by including several indices (16-49% for SMB and 21-30% for melting). As anticipated by the Reviewer, this indicates an interplay between the different modes of variability. A column providing the correlation of the multi-linear regression has been added to Tables 3 and 4, with associated description in section 3.2, L.464-468.

Even with SOI instead of NINO34 and considering multi-linear relationships, the part of explained variance never exceeds 50% of the summer melt and SMB variance. Possible reasons for this are (i) the modes of variability do not explain all the variance locally; for example, the leading EOF of SST in the Equatorial Pacific (representing ENSO) only accounts for 50 to 70% of the SST variance (e.g. Roundy, JCLI 2015), meaning that the tropical convection thought to influence Antarctica is not completely described by SOI or NINO34; (ii) assuming that a large part of the tropospheric circulation variability is explained by ENSO, SAM and ASL indices, there are reasons why the connection may be weaker for SMB and surface melting because of their non-linear dependence on sea ice and evaporation in coastal regions, the evolution of snow properties, etc; (iii) strong modulation of the southeast Pacific extratropical circulation by Rossby wave train is not only due to the existence of El Niño events but also depends on the exact spatial distribution of deep convection in the tropical central Pacific and to the strength of the polar jet (Harangozo et al. 2004) (iv) a part of the variability of SMB and melting may

be stochastic, i.e. not necessarily driven by variability with spatio-temporal coherence at large scales. We have added a paragraph in the text (section 3.2 L.492-509) to mention these possible reasons for relatively little explained variance.

The postulation of potential lags is not adequately investigated. The hypothesis regarding sea ice reduction and transport from the Ross Sea could be tested as MAR using the sea-ice concentration from ERA-Interim. Thus, please consider adding analysis of sea ice concentrations to support this postulation. Although not as clear cut, intrusion of marine CDW could be evaluated by looking at the effective wind stresses as done by Steig et al. just off the continental shelf and attempt to quantify a six-month lag between strong wind events and surface melt. Also, there is no mention of potential preconditioning of the snowpack/firn for melt. An additional important variable in control of surface melt in the summer is the amount of snow that fell the prior winter, and it should be added to the analysis presented and included in Table 4. This signal might not matter at all, but also could lead to misinterpretation of an ENSO lag. Please consider all potential snowpack preconditioning variables that might explain melt from year-to-year.

In the discussion, we indeed suggested the existence of a delayed response of summer SMB and surface melting to the previous winter's ENSO events. We are not able to show perfectly robust evidence because this would probably require running dedicated experiments using a global ocean/atmosphere model (e.g. pacemaker simulations in Holland et al. 2019). We have nonetheless expanded this part of the discussion based on the literature and on additional diagnostics that indicate that such physical lag is highly probable:

1- Seasonality of ENSO and Rossby wave trains: First of all, the connection between ENSO and the Amundsen sector are thought to occur through Rossby wave trains originating in the equatorial Pacific (e.g. Ding et al. 2011). Numerous observational and modeling papers reported that austral winter and spring conditions were more favorable for Rossby wave trains to be formed and to propagate to high southern latitudes (Harangozo 2004, Lachlan-Cope and Connolley 2006, and references therein). Scott Yiu and Maycock (2019) have recently found that the poleward propagation of tropically sourced Rossby waves in summer is inhibited by the strong polar front jet in the South Pacific sector at that time of the year, which leads to Rossby wave reflection away from the Amundsen Sea region. Steig et al. (2011) also found that changes in wind stress over the Amundsen Sea had non-significant correlations to ENSO indices in austral summer, in contrast to the other seasons showing significant correlations.

2- Snow memory: In the initial draft, we only mentioned that there was no correlation between summer melt rates and snow temperature in the previous months (which could be hypothesized as El Niño events are known to warm West Antarctica in winter; Ding et al. 2011). We agree with Reviewer #1 that snowfall in winter and spring could also be thought to influence summer melt (e.g. because the amount of fresh snow affects albedo feedbacks). However, in all the



basins, we find no significant correlations between summer melt rates and snow accumulated over the previous 3 months or 6 months. For example, here are some correlation values (R):

Thwaites:

R (DJF melt / DJF smb) = 0.31 (p=0.06)  
R (DJF melt / SON smb) = -0.03 (p=0.86)  
R (DJF melt / JJA+SON smb) = -0.01 (p=0.94)

Pine Island:

R (DJF melt / DJF smb) = 0.48 (p=0.02)  
R (DJF melt / SON smb) = -0.21 (p=0.19)  
R (DJF melt / JJA+SON smb) = -0.11 (p=0.50)

Dotson:

R (DJF melt / DJF smb) = 0.48 (p=0.01)  
R (DJF melt / SON smb) = 0.09 (p=0.59)  
R (DJF melt / JJA+SON smb) = 0.11 (p=0.53)

We conclude that the lag between ENSO and melt rates is not explained by preconditioning of the snowpack in previous seasons.

3- Ocean/sea-ice memory: If the lag is not explained by snow, then it has to be explained by the other slow media, i.e. the ocean/sea-ice system. Here also, the literature provides some indications. First of all, Clem et al. (2017) mentioned stronger lagged correlation between SON ENSO and DJF sea ice cover than synchronous correlation in DJF. This lag relationship was shown to affect DJF surface air temperatures over West Antarctica (warmer for El Niño phases). Pope et al. (2017) found that El Niño events developing in MAM created a dipole of sea ice anomalies, with decreased (increased) concentration in the Ross Sea (Amundsen and Bellingshausen Seas). Using a novel sea ice budget analysis, they showed that the decreased concentration in the Ross Sea was then advected eastward, reaching the Amundsen Sea in SON and DJF.

There is also another possible pathway for lagged ENSO/sea-ice relationship. The zonal wind stress over the Amundsen Sea continental shelf break is a good proxy for the transport of Circumpolar Deep Water (CDW) onto the continental shelf (Thoma et al. 2008; Holland et al. 2019). Steig et al. (2012) noted significant correlations between that wind stress and ENSO in JJA and SON but not in DJF. All these studies pointed out scales of a few months for the build up and advection of CDW on the continental shelf then into the ice shelf cavities where they produce basal melting. As stronger ice-shelf melt rates tend to decrease sea ice in this region due to the entrainment of warm CDW towards the surface (Jourdain et al. 2017; Merino et al. 2018), this deep ocean pathway may also explain a part of the lag between ENSO and DJF sea ice in the Amundsen Sea.

To complement these analyses, we have added a composite of DJF sea ice cover anomalies for El Niño events in JJA (6-month lag Fig.14). This composite is dominated by a significant negative anomaly, confirming that ENSO in austral winter has a significant effect on sea ice 6 months later, which could arguably explain the increase in humidity and favor high melt rates and high SMB. There are several possible reasons for such a lag, it could be related to the slow advection of winter sea ice anomalies from the Ross Sea, or to the slow advection of ocean temperature anomalies (CDW) towards the ice shelves then towards the surface through the meltwater pump, but we leave the quantification of these aspects for future research.

Minor Comments :

Line 16 – change to “Amundsen Sea glaciers”

Done

Line 58 – change “underlaying” to “underlying”

Done

Line 114 – remove the ‘;’ at the beginning of the line

Done

Line 140 – change “estimates” to “estimate”

Done

Line 185-186 – remove the sentence “These data were collected over the Thwaites and Pine Island basins.” as it is redundant with Lines 181-182.

Done

Section 2.3 : Are these indices derived from ERA-Interim for consistency with the MAR output? If not, please state that and justify their use.

We have added this information in section 2.3

Line 273 – Are “overestimate” and “underestimate” confused? Shouldn’t it be “The model tends to underestimate and overestimate highest and lowest wind speeds”?

We agree with the Reviewer’s comments and this has been modified.

Line 299 – Remove “(Medley et al. 2013, 2014)” as it is already mentioned in the sentence.

Done

Line 382 - add “is” after “mechanism”

Done

Figure 10/11 – Please add in the legend that blue represents moisture convergence for clarity.

Figure 10 and 11 have been changed, we now choose to show the Integrated Vapor Transport instead of humidity convergence following concerns from reviewer #2 and D. Bromwich.

Paragraph beginning with 530 – Perhaps it is important to mention here that DJF makes up the smallest percentage of annual accumulation, so it is not surprising that the findings do not match Medley and Thomas.

Done

---

### **Interactive comment by Anonymous Referee #2**

This paper presents results from the regional climate model MAR run for the Amundsen Sector of West Antarctica. The paper is well written and thorough, although some parts the paper needs improvement.

After reading the paper and collecting my points of concerns, I've read the other review and the comment of David Bromwich. I agree with their major concerns and these concerns have to be addressed. Additionally, I have the following major comments:

It needs to be addressed why SMB summer is discussed and not the annual SMB. I can imagine a reason, but this - or any other - reason is not given.

We thank Reviewer #2 for these constructive and motivating feedbacks. As for Reviewer#1 we agree with most of the objections and have considered them in the revised manuscript. As detailed in our response to Reviewer #1, we have added an explanation on why we focused on summer SMB (now in section 1).

Although the patterns in Figures 8-12 are logic and reasonable, its worrisome that most of the signals showed are insignificant. Try to get a better understanding of the significance. For example, for geopotential fields the gradient matters more than the value, so you might take a “relative elevation” approach similar to the ASL central pressure. You might also try a different method to determine significance, for example, bootstrapping. If the patterns remain mostly insignificant it implies that the shown patterns do occur during high/low melt/SMB but not necessarily lead to high/low melt/SMB.

We first would like to point out that all the composites showed a clear significant area over the coastal region of the Amundsen Sea and over the studied drainage basins, to the exception of the 700 hPa geopotential height and the humidity divergence at 850 hPa. We thank the Reviewer for his suggestion that the mean geopotential height matters less than the gradient.

To circumvent this issue, we have added the composite by analyzing the geopotential pattern divided by the domain-averaged value for each DJF season. This produces much more significance than in the initial version, as shown in the modified Fig. 9 and Fig. 12. See next comment for the case of humidity divergence.

I'm not convinced that humidity convergence @ 850 hPa is the best parameter to show. For SMB anomalies: As the moisture holding capacity of air is not that big, the convergence is directly linked to precipitation generation. Added compared to SMB is a whole bunch of noise due to variations in the elevation of the 850 hPa level and noise is added by apparently near stationary numerical waves. I would be more interested to see anomalies in the temperature @ 700 hPa / 850 hPa and vertical integrated moisture content fields. For melt anomalies: it likely boils down to that high melt years have also higher summer SMB although this relation might not be significant. Furthermore, the authors do show that cloudiness increases, but fail to prove that this is the only cause. To which extent is the higher melt due to cloudiness and which extent due to advection of warmer air? What is the anomaly of temperatures at 700 hPa? This anomaly can be easily included in Figures 12 a,b. I know temperature and cloudiness anomalies are likely covarying, so disentangling might be complicated. Helpful might be the MSSA technique (Plaut and Vautard, 1994; Allen and Robertson, 1996).

We agree that the divergence of humidity transport was too noisy and, in the end, little supportive of our mechanism. We have replaced this diagnostic by the integrated vapor transport (IVT) that is calculated as:

$$IVT = \int_{925}^{700} qv \frac{dP}{g}$$

where  $v$  is the velocity along the y-axis and  $g$  the gravity parameter. We have replaced humidity divergence composites by IVT composites in Fig.10 and Fig.11. It clearly shows that high SMB and high melt rates are linked to a strong southward vapor transport towards the drainage basins of the Amundsen Sea. The arrival of this vapor from the mid-latitude into the colder Antarctic region can arguably induce condensation and cloud formation.

We have also looked at the composite of sensible heat fluxes (this has been added to the supplementary material) versus longwave downward heat fluxes. The sensible heat flux is negative for the high-melt composite, which means that energy is going from the snow surface to the air (the temperature of the snow surface is higher than the temperature of the air above), so advection of warm air above the surface is not responsible of higher surface melt. Therefore, as suggested in our initial manuscript, changing downward longwave heat flux is the main mechanism for low/high surface melt events. Increase in cloudiness and humidity transport is therefore the main driver. We have added a comment on this in section 3.2, L. 418-419. Fig.10 and Fig.11 has been changed. (Figure below has been added to supplementary material)

(line 527): CDW intrusions cannot be proven directly with the data from this manuscript (although SSTs and wind stress are available), but sea ice anomalies are available. It takes only a few steps to verify if the hypotheses are confirmed by data, so take those steps. And if the data does not confirm this hypothesis, that must be stated as well.

See our response to Reviewer #1: we have substantially expanded our discussion of this hypothesis based on further literature review and on an additional DJF sea ice composite for JJA Niño events. Although providing perfectly robust evidence of causality would require specific AOGCM experiments, we believe that several lines of evidence indicate that such physical lag is highly probable.

Minor comments :

158: The sentence on the boundary relaxation is ambiguous: It could also mean that every 6 hours the state in at the boundaries “is forced back” to ERA-Interim values. However, I presume that every time step fields are relaxed to ERA-Interim fields with 6- hourly temporal resolution. Rephrase to remove this ambiguity. Furthermore, add the boundary relaxation zone to the graph by using shading or something else and explain in the text how wide this zone was. From eg Fig 10 I conclude it was rather narrow, explain why or add a reference.

Explanation about boundary relaxation has been changed, as well as Fig.1 where relaxation zone is now shown in white. Fig.10 has been change related to next comments.

131: polar-oriented. Did you mean “polar adapted”? Oriented is not wrong but uncommon in this meaning.

Done

224: I would prefer if these webpage-links could be included as references so that the text becomes less disturbed. But that’s up to Copernicus to solve/decide on.

We followed the manuscript preparation guidelines for authors (webpage, references)

298: How this performance compares to other studies, thus MAR-full Antarctica and various RACMO2 products? Add a comment on this in the text.

We have added a comment in section 3.1 L-287.288. Compared to MAR-full Antarctica we present very similar biases (Agosta et al., 2019), correlation for SMB compared to observation (Glacioclim SAMBA).  $R=0.95$  for our simulation and  $R=0.93$  for MAR-full Antarctica, same for bias of 0.13 and 0.14 for MAR-full Antarctica. This improvement is not really significant and can be explained only by higher resolution and higher spatial variability in our simulation. Comparison with RACMO2 products is beyond the scope of our studies and will be the subject of future studies.

321: It might be interesting to make a scatter plot of the modelled and interpolated QuickScat melt for their overlapping time period. You could color code the dots per ice shelf or drainage

basin and even add regression lines per drainage basin. You don't discuss the few spots in West Antarctica where MAR gives high melt rates – do this. And have a look at <https://www.the-cryosphere.net/13/1473/2019/tc-13-1473-2019.pdf> if this might be a possible explanation for your model deviations too.

We agree we have added scatter plot (Fig.6) and related discussion L.336-337.

359: It would be nice if these high/low SMB/melt years as listed, maybe by adding symbols in figure 7.

We have added a table in supplementary material (Tab.S4) and not in Fig.7 because composite dates correspond to values with low/high SMB/Melt only over Thwaites and Pine Island basins and not over the model domain as explained in section 3.2 “For a sake of clarity, we only consider the Pine Island and Thwaites basin (together) as a first approach. “

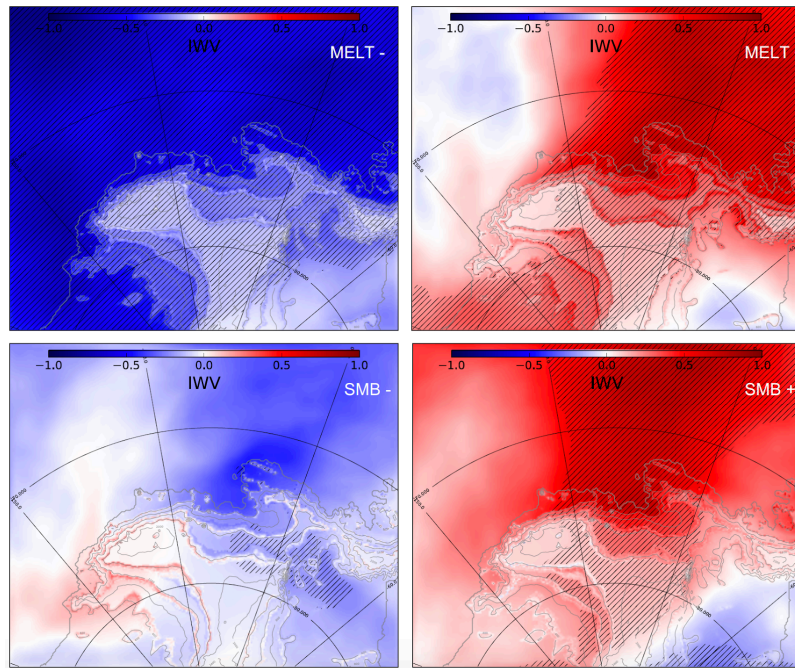
363: In Figure 8 your plotting two differences per frame – that makes it harder to include signs of significance. Are these differences significant? Make a comment in the text and, if possible, find a way to display if deemed relevant.

Fig.8 does not represents differences (composite - climatology) like other composite as the climatology is shown in grey and composite in color, we choose to plot all in the same panel as the comparison of both the high and low composites with the climatology are necessary.

378: Cloud cover could be a poorly performing parameter – I know models in which this is the case. Verify if you find similar/equivalent patterns in the vertical integrated cloud content (please add these figures in the rebuttal letter) and state in the manuscript if similar / equal patterns are found in the vertical integrated cloud content.

We have added IVT (integrated vapor transport) in Fig.10 and Fig.11 and here is the composite for integrated water vapor ( $\text{kg m}^{-2}$ ):





379: As snowfall exceeds the SMB due to sublimation, the “95%” in the quote is a bit odd. Rephrase.

Done

425-427: This is not necessarily true. If positive SMB anomalies occur only if NINO34 is positive and ASL-longitude is negative, then their impact on SMB is not unrelated even though NINO34 and ASL-longitude are unrelated themselves

We do not understand the reviewer's concern with our sentence ("NINO34 and the ASL longitudinal location are not significantly connected together (Table 1), therefore their connection to SMB can be considered as independent from each other"). In the example given by the reviewer, both ENSO and the ASL migration impact SMB, but both act through independent connections (assuming linear relationships, i.e. perfectly described by correlations). It does not mean that the coincidental phases of the two indices do not explain the strongest SMB events.

438: Would it not be more straightforward to see if there is a correlation between SMB and melt rates? And if not, state this.

See our response to the major comments by Reviewer#1

Table S1: Add the numbers used in Fig 1 to the table – Yes, I know they are ordered from 1 to 41, but adding the number makes it just a slightly bit easier

We agree, this has been done

Fig 1: Consider to include excluded AWS stations in the figure using a different color, as long as they are on the map. Names are not needed.

We think that display the 243 AWS can disturb the understanding of the figure, so we have not followed this suggestion.

Fig 2: The lines are not explained in the figure caption. Are the lines derived using normal fitting or perpendicular fitting techniques? Colors are not different enough to identify stations in the graph, so either use more distinguishable colors or simply don't try: give all lines the same color.

We use least-mean-square fit (linregress in python) we have added this information within the caption.

A drawback of a dot-plot is that you can't see differences in density once the dots form a continuous cloud. It might be worth the work to calculate the dot-density per (e.g.) 0.01 C-squared (Fig 2a) and plot this point density as contour graph on top of the dots. This added information on the point-density would make a statement like line 273-274 visible from the graph, the overestimation for low wind speeds is not well visible in the point cloud.

We have changed Fig.2 and have added transparency on dots in order to see density differences. We have kept stations names (some might it useful) but we have changed colors (less transparent, more distinguishable). Legend has been changed and fitting method explained.

Fig 3: I'm not fond of the graphical solution to plot SMB in greyscale – details are hardly visible nor quantifiable. For example, I have no clue what the magnitude of the SMB from MAR is near the Medley data. Replace the grey by colors and add the basin delineation in a different manner. In all solutions, more detail must become visible for SMB ranging from 200 to 500 mm w.e. per year.

We agree and we have changed Fig.3 (colormap, and range).

Fig 5: Replace the grey by clear colors and extend the scale to higher values than 100 mm w.e. per year – this should be obvious as you do discuss these high melt values in the main text.

We agree with this comment and we have changed the grey colors. As far as the color bar is concerned, we discuss high melt values but only over Thwaites and Pine Island, that's why we choose a color bar where differences in melt rate over Thwaites and Pine Island are distinguishable.

Fig 9: Contours in b are labelled with 0-2-5-8 intervals, but their regular spacing looks like 0-2.5-5-7.5. Check this. Hatching is not explained – should be done here too. Hatching line thickness varies with viewer.

Fig.9 has been changed and contours checked. We have added hatching explanation.

Plaut, G., and R. Vautard, 1994: Spells of low-frequency oscillations and weather regimes in the Northern Hemisphere. *J. Atmos. Sci.*, 51, 210–236, doi:<https://doi.org/10.1175>

Allen, M. R., and A. W. Robertson, 1996: Distinguishing modulated oscillations from coloured noise in multivariate datasets. *Climate Dyn.*, 12, 775–784, doi:<https://doi.org/10.1007>

---

### **Interactive comment by David Bromwich**

This is a comprehensive analysis.

[We thank David Bromwich for these comments that have pushed us to improve our manuscript.](#)

One major shortcoming is that it really underplays the comparisons of the present results with those obtained by Deb et al. (2018) also based on regional climate modeling for 1979-2015 summers where a leading conclusion is: "El Niño episodes during austral summer drive warmer conditions over Amundsen Sea Embayment ice shelves that cause enhanced surface melting". El Niño influences play a relatively minor role in the current analysis. The explanation likely lies in the discussion on lines 475-486.

[Deb et al. \(2018\) was cited 4 times in the submitted manuscript, but going back to our text, we agree that there should be more comparison to the results obtained by Deb et al. \(2018\) about the connections to ENSO and the ASL. We have added that “The relationship between ENSO and the number of melt days was identified by Deb et al. \(2018\) using both regional simulations and a satellite product”. Our results are difficult to compare more quantitatively because different methods and metrics were used in Deb et al. \(2018\) and in our study. We now also mention that “longitudinal migrations of the ASL are not the main driver of surface melting variability, as previously noted by Deb et al. \(2018\)”.](#)

I didn't think the analysis for a lagged relation between El Niño forcing SMB/melting (Fig. 13) to be very compelling, at best possible.

[See our response to Reviewer #1: we have substantially expanded our discussion of this hypothesis based on further literature review and on an additional DJF sea ice composite for JJA Niño events. Although providing perfectly robust evidence of causality would require specific AOGCM experiments, we believe that several lines of evidence indicate that such physical lag is highly probable.](#)

I don't understand what is meant by humidity divergence (Figs. 10 and 11). Normally one evaluates moisture transport divergence in relation to P-E. Please clarify.

We apologize for the lack of clarity and we did plot the moisture transport divergence. We have nonetheless decided to show the meridional integrated vapor transport instead of the divergence, which better shows the moisture transport from the mid-latitudes to the Antarctic ice sheet.

References that were not cited in the initial draft:

Clem, K. R., Renwick, J. A., and McGregor, J. (2017). Large-scale forcing of the Amundsen Sea Low and its influence on sea ice and West Antarctic temperature. *Journal of Climate*, 30(20), 8405-8424.

Ding, H., Greatbatch, R. J., and Gollan, G. (2014). Tropical influence independent of ENSO on the austral summer Southern Annular Mode. *Geophysical Research Letters*, 41(10), 3643-3648.

Harangozo, S. A. (2004). The relationship of Pacific deep tropical convection to the winter and springtime extratropical atmospheric circulation of the South Pacific in El Niño events. *Geophysical research letters*, 31(5).

Holland, P. R., Bracegirdle, T. J., Dutrieux, P., Jenkins, A., and Steig, E. J. (2019). Climate Forcing of the West Antarctic Ice Sheet: Anthropogenic Trends and Internal Climate Variability. *Nature Geoscience*.

Lachlan-Cope, T. and Connolley, W. (2006). Teleconnections between the tropical Pacific and the Amundsen-Bellinghausens Sea: Role of the El Niño/Southern Oscillation. *Journal of Geophysical Research: Atmospheres*, 111(D23).

Roundy, P. E.: On the Interpretation of EOF Analysis of ENSO, Atmospheric Kelvin Waves, and the MJO, *J. Climate*, 28(3), 1148–1165, doi:10.1175/JCLI-D-14-00398.1, 2014.

Scott Yiu, Y. Y. and Maycock, A. C. (2019). On the seasonality of the El Niño teleconnection to the Amundsen Sea region. *Journal of Climate*.

Thoma, M., Jenkins, A., Holland, D. and Jacobs, S. (2008). Modelling circumpolar deep water intrusions on the Amundsen Sea continental shelf, Antarctica. *Geophysical Research Letters*, 35(18).

# Interannual Variability of Summer Surface Mass Balance and Surface Melting in the Amundsen Sector, West Antarctica

Marion Donat-Magnin<sup>1</sup>, Nicolas C. Jourdain<sup>1</sup>, Hubert Gallée<sup>1</sup>, Charles Amory<sup>3</sup>, Christoph Kittel<sup>3</sup>, Xavier Fettweis<sup>3</sup>, Jonathan D. Wille<sup>1</sup>, Vincent Favier<sup>1</sup>, Amine Drira<sup>1</sup>, Cécile Agosta<sup>2</sup>.

<sup>1</sup>Université Grenoble Alpes/CNRS/IRD/G-INP, IGE, 38000, Grenoble, France  
<sup>2</sup>Laboratoire des Sciences du Climat et de l'Environnement, IPSL/CEA-CNRS-UVSQ UMR 8212, CEA Saclay, F-91190, Gif-sur-Yvette, France  
<sup>3</sup>F.R.S.-FNRS, Laboratory of Climatology, Department of Geography, University of Liège, B-4000 Liège, Belgium

Correspondence to: Marion Donat-Magnin (marion.donatmagnin@gmail.com)

## Abstract.

Understanding the interannual variability of Surface Mass Balance (SMB) and surface melting in Antarctica is key to quantify the signal to noise ratio in climate trends, identify opportunities for multi-year climate predictions, and to assess the ability of climate models to respond to climate variability. Here we simulate summer SMB and surface melting from 1979 to 2017 using the regional atmospheric model MAR at 10 km resolution over the drainage basins of the Amundsen Sea glaciers in West Antarctica. Our simulations reproduce the mean present-day climate in terms of near-surface temperature (mean overestimation of 0.10 °C), near-surface wind speed (mean underestimation of 0.42 m s<sup>-1</sup>), and SMB (relative bias < 20% over Thwaites glacier). The simulated interannual variability of SMB and melting is also close to observation-based estimates.

For all the Amundsen glacial drainage basins, the interannual variability of summer SMB and surface melting are driven by two distinct mechanisms: high summer SMB tends to occur when the Amundsen Sea Low (ASL) is shifted southward and westward, while high summer melt rates tend to occur when ASL is shallower (i.e. anticyclonic anomaly). Both mechanisms create a northerly flow anomaly that increases moisture convergence and cloud cover over the Amundsen Sea and therefore favors snowfall and downward longwave radiation over the ice sheet. The part of interannual summer SMB variance explained by the ASL longitudinal migrations increases westward and reaches 40% for Getz. Interannual variation of the ASL relative central pressure is the largest driver of melt-rate variability, with 11 to 21% of explained variance (increasing westward). While high summer SMB and melt rates are both favored by positive phases of El Niño Southern Oscillation (ENSO), the Southern Oscillation Index (SOI) only explains 5 to 16 % of SMB or melt rates interannual variance in our simulations, with moderate statistical significance. However, the part explained by SOI in the previous austral winter is greater, suggesting that at least a part of the ENSO-SMB and ENSO-melt relationships in summer is inherited from the previous austral winter. Possible mechanisms involve sea-ice advection from the Ross Sea and intrusions of circumpolar deep water combined with melt-induced ocean overturning circulation in ice-shelf cavities. Finally, we do not find any correlation with the Southern Annular Mode (SAM) in summer.

Supprimé: 2

Supprimé: 8

Supprimé: NINO34

## 1 Introduction

From 1992 to 2017, the Antarctic continent has contributed  $7.6 \pm 3.9$  mm to the global mean sea level (Shepherd et al., 2018) and this contribution may increase over the next century (Ritz et al., 2015; DeConto and Pollard, 2016; Edwards et al., 2019). The recent mass loss from the Antarctic ice sheet is dominated by increased ice discharge into the ocean (Shepherd et al., 2018), but both surface mass balance (SMB) and ice discharge may significantly affect the Antarctic contribution to future sea level rise (Asay-Davis et al., 2017; Favier et al., 2017; Pattyn et al., 2018). Despite recent improvements of ice-sheet models motivated by newly available satellite products over the last 10-20 years, large uncertainties remain in both the SMB and ice dynamics projections, hampering our ability to accurately predict future sea level rise (Favier et al., 2017; Shepherd and Nowicki, 2017).

Largest ice discharge changes in Antarctica are observed in the Amundsen sector with an increase of 77% over the last decades (Mouginot et al., 2014). Current changes in the dynamics of glaciers flowing into the Amundsen Sea are dominated by ocean warming rather than changes in surface conditions over the ice sheet (Thoma et al., 2008; Pritchard et al., 2012; Turner et al., 2017; Jenkins et al., 2016, 2018). Increased oceanic melting can trigger marine ice sheet instability, leading to increased ice discharge, thinning ice, and retreating grounding lines (Weertman, 1974; Schoof, 2007; Favier et al., 2014; Joughin et al., 2014). In parallel, increased surface air temperature can lead to surface melting, subsequent hydrofracturing, and possibly to major thinning and retreat of outlet glaciers after the collapse of ice shelves (DeConto and Pollard, 2016). Surface melting, leading to meltwater ponding, drainage into crevasses and hydrofracturing, is thought to be the main **cause of** the Larsen ice shelves collapse over the last decades in the Antarctic Peninsula (van den Broeke, 2005; Scambos et al., 2009; Vaughan et al., 2003). While surface melting is currently limited to relatively rare events over the Amundsen Sea ice shelves (Nicolas and Bromwich, 2010; Trusel et al., 2012) and **underlying** reasons for melt ponds formation versus active surface drainage network remains unclear (Bell et al., 2018), the rapid surface air warming observed (Steig et al., 2009; Bromwich et al., 2013) and projected (Bracegirdle et al., 2008) in this region suggests that surface melting could increase in the future. Our study focuses on the two atmospheric-related aspects that can significantly affect the contribution of the Amundsen Sea sector to sea level rise, i.e., **snowfall** accumulation that is expected to increase in a warmer climate and therefore to reduce the mean sea level, and surface melting that could potentially induce more ice discharge and therefore increase the mean sea level.

Understanding the interannual variability of SMB and surface melting is key to (i) quantify the signal to noise ratio in climate trends, (ii) identify opportunities for seasonal predictions, and (iii) assess the capacity of climate models to respond to global climate variability. Furthermore, years with particularly strong surface (or oceanic) melting could trigger irreversible grounding line retreat without the need for a long-term climate trend. Interannual variability in the Amundsen Sea region is usually described in

Supprimé: responsible for

Supprimé: underlying

Supprimé: . Snowfall



terms of connections with the El Niño Southern Oscillation (ENSO), the Southern Annular Mode (SAM), and the Amundsen Sea Low (ASL). Our study revisits these connections through dedicated regional simulations based on the MAR model (Fettweis et al., 2017; Agosta et al., 2019). Hereafter, we start by reviewing recent literature on these climate connections.

The El Niño Southern Oscillation (ENSO ; Philander et al., 1989) is the leading mode of ocean and atmosphere variability in the tropical Pacific. It is the strongest climate fluctuation at the interannual timescale and can bring seasonal to multi-year climate predictability (e.g. Izumo et al., 2010). Global climate models predict an increasing number of extreme El Niño events in the future, with large global impacts (Cai et al., 2014, 2017). Interannual and decadal variability in the tropical Pacific affects air temperature (Ding et al., 2011), snowfall (Bromwich et al., 2000; Cullather et al., 1996; Genthon and Cosme, 2003), sea ice extent (Pope et al., 2017; Raphael and Hobbs, 2014) and upwelling of circumpolar deep water favoring ice-shelf basal melting (Dutrieux et al., 2014; Steig et al., 2012; Thoma et al., 2008) in West Antarctica. Recent studies found concurrences between El Niño events and summer surface melting over West Antarctic ice shelves (Deb et al., 2018; Nicolas et al., 2017; Scott et al., 2019). These connections are generally explained in terms of Rossby wave trains excited by tropical convection during El Niño events and inducing an anticyclonic anomaly over the Amundsen Sea (Ding et al. 2011). Paolo et al. (2018) reported a positive correlation between ENSO and the satellite-based ice-shelf surface height in the Amundsen Sea over 1994-2017. Based on a detailed study of the extreme El Niño/La Niña sequence from 1997 to 1999, these authors suggested that El Niño events could increase snow accumulation but, also increase ocean melting even more, thus leading to an overall ice shelf mass loss. The impact of ENSO was found to be stronger for the Dotson ice-shelf and eastward, and weaker for Pine Island and Thwaites (Paolo et al., 2018). However, the aforementioned studies were based on the analysis of few recent ENSO events, and did not account for the highly-variable properties of ENSO over multi-decadal periods (e.g. Deser et al., 2012; Newman et al., 2011).

The Southern Annular Mode (SAM; Hartmann and Lo, 1998; Limpasuvan and Hartmann, 1999; Thompson and Wallace, 2000) is the dominant mode of atmospheric variability in the Southern hemisphere, and corresponds to a variation of the strength and position of the circumpolar westerlies. Over the last three to five decades, the SAM has exhibited a positive trend, i.e., westerly winds have been strengthening and shifting poleward (Chen and Held, 2007; Jones et al., 2016; Marshall, 2003). Medley and Thomas (2019) found similar patterns for the SAM trends and the reconstructed snow accumulation trend over 1801-2000. By contrast, the temperatures above the melting point over the Amundsen ice shelves were found to be largely insensitive to the polarity of the SAM (Deb et al., 2018). The SAM phase has also been suggested to influence the ENSO teleconnection to the south Pacific: in-phase ENSO and SAM events (i.e. El Niño/SAM- or La Niña/SAM+) favor anomalous transient eddy momentum fluxes in the Pacific that make the ENSO teleconnection to the South Pacific stronger than average (Fogt et al., 2011).

Supprimé: even more

Supprimé: encountered

115 The Amundsen sea low (ASL ; Raphael et al., 2016; Turner et al., 2013a) is a dynamic low-pressure system located in the Pacific sector of the Southern Ocean and moving across the Ross, Amundsen, and Bellingshausen seas. The ASL is important regionally and variations of its central pressure and position respectively reflect the second and third leading modes of the Southern hemisphere climate respectively (Scott et al. 2019 their figure 3). A westward shift of the ASL induces northerly flow anomalies over the  
120 Amundsen Sea, leading to warmer conditions and increased moisture transport over the ice sheet (Hosking et al., 2013; Thomas et al., 2015; Hosking et al., 2016; Raphael et al., 2016; Fyke et al., 2017). Variations in the ASL central pressure also largely impact the West Antarctic climate: anti-cyclonic anomalies near 120°W lead to marine air intrusion over the ice sheet, thereby increasing cloud cover, longwave downward radiations and therefore surface air temperature over WAIS (Scott et al., 2019).  
125 While a deepening of the ASL is predicted for the twenty-first century in response to greenhouse gas emissions, its high regional variability makes future changes of the ASL difficult to predict (Hosking et al., 2016; Turner et al., 2009).

Supprimé: ;

Importantly, ENSO and SAM are not independent from each other and both modes of climate variability impact the ASL (Fogt and Wovrosh, 2015). SAM influences the ASL central pressure since it affects the mean sea level pressure over Antarctica (Turner et al., 2013a). The second and third leading modes of variability in the South Pacific have been suggested to be affected by Rossby wave trains induced by tropical convection anomalies (Mo and Higgins, 1998). In terms of ASL, it corresponds to a migration further west (east) during the La Niña (El Niño), but the difference has a low statistical significance (Turner et al., 2013b). Scott et al. (2019) recently reported that El Niño conditions favored  
135 blocking in the Amundsen Sea as well as a negative SAM phase, both leading to warm surface air anomalies in West Antarctica.

Supprimé: SAM influences the ASL central pressure since it affects the mean sea level pressure over Antarctica (Turner et al., 2013a)

\_\_\_\_ In this study we revisit the influence of ENSO, SAM and ASL on summer SMB and melting over the drainage basins of the Amundsen sector in West Antarctica for the 1979-2017 period. While the summer focus on melt rates is obvious, SMB in DJF only represents 15% of the annual SMB. It is nonetheless interesting to analyze the similarities and differences in what drives SMB and melting, and the modes of variability and their teleconnections to the Amundsen Sea region both have strong seasonal characteristics, so that each season needs to be considered separately. To do so, we simulate the surface conditions of the Amundsen Sea region over 1979-2017 using the polar-adapted regional atmospheric  
140 model MAR forced by the ERA-Interim reanalysis. Section 2 describes the methodology followed in the study and presents the model and observations used for comparison. The model results are analyzed and evaluated against observations in Section 3, after evaluating the model skills (section 3.1), we analyze and discuss our results on the potential impact of large-scale climate variabilities on the SMB and melting  
145 in section 3.2 and 4. The conclusions are provided in Section 5.

Supprimé: oriented

2.1 Model

To ~~estimate~~ SMB and surface melt over the Amundsen sector we use the regional atmospheric model MAR (Gallée and Schayes, 1994) and specifically the version 3.9.3 (<http://mar.cnrs.fr>, last access: ~~25 September~~ 2019). The model solves the primitive equations under the hydrostatic approximation. It solves conservation equations for specific humidity, cloud droplets, rain drops, cloud ice crystals and snow particles (Gallée, 1995; Gallée and Gorodetskaya, 2010). MAR represents coupled interactions between the atmospheric surface boundary layer and the snowpack using the Soil Ice Snow Vegetation Atmosphere Transfer (SISVAT) originally developed by De Ridder and Gallée (1998). The snow–ice part of SISVAT includes submodules for surface albedo, meltwater percolation and refreezing, and snow metamorphism based on an early version of the CROCUS model (Brun et al., 1992). MAR has been largely evaluated in polar regions (e.g. Amory et al., 2015; Gallée et al., 2015; Lang et al., 2015; Fettweis et al., 2017; Kittel et al., 2018; Agosta et al., 2019; Datta et al., 2019).

Our domain includes the drainage basins of the Amundsen glaciers and a large part of the Amundsen Sea until 65°S. It covers an area of 2800 x 2400 km at 10 km horizontal resolution (Fig. 1) and 24 vertical sigma levels located from approximately 1 m to 15500 m above the ground. We use 30 snow layers, resolving the 20 first ~~meters~~ of the snowpack, with a fine vertical resolution at the surface (1 mm) increasing with depth, snow layer thickness varies dynamically depending on the physical properties of overlying snow layer properties. ~~If neighboring layers get similar properties then layers are associated together.~~ The radiative scheme and cloud properties are the same as in Datta et al. (2019) and the surface scheme including snow density and roughness are the same as in Agosta et al. (2019). ~~The model is forced by ERA-interim reanalysis (Dee et al., 2011), which performs well over Antarctica (Bromwich et al., 2011; Huai et al., 2019), at 6 hourly temporal resolution and relaxed over ~400km laterally (pressure, wind, temperature, specific humidity, the relaxation zone is shown in Fig. 1), at the top (i.e. above 10 km) of the troposphere (temperature, wind), and at the surface (sea ice concentration, sea surface temperature).~~ The Bedmap2 surface elevation dataset is used for the ice-sheet topography (Fretwell et al., 2013). The snowpack density and temperature are initialized from the pan-Antarctic simulation from Agosta et al. (2019). ~~Drifting snow is relatively infrequent in the Amundsen region (Lenaerts et al., 2012) so that the drifting snow module has been switched off in our configuration, similarly as in Agosta et al. (2019).~~

In section 3.2 we provide the SMB constituents averaged over individual drainage basins.

185

2.2 Antarctic surface observations

We make use of meteorological data from the SCAR database including observations from the Italian Antarctic Research Program (<http://www.climantartide.it>, last access: ~~25 September~~ 2019), the Antarctic

Supprimé: estimates

Supprimé: meter

Supprimé: , if

Supprimé: The model is 6 hourly forced laterally (pressure, wind, temperature, specific humidity), at the top (i.e. above 10 km) of the troposphere (temperature, wind), and at the surface (sea ice concentration, sea surface temperature) by the

Supprimé: .

Supprimé: Drifting snow is relatively infrequent in the Amundsen region (Lenaerts et al., 2012)

Supprimé: 14 May

200 Meteorological Research Center (AMRC program) (<http://amrc.ssec.wisc.edu/>, last access: 25 September 2019) and the Australian Antarctic automatic weather station (AWS) dataset (<http://aws.acecrc.org.au/>, last access: 25 September 2019). Among the 243 AWS available over Antarctica since 1980, we selected stations located no more than 15 km from the closest continental MAR grid point. For each location, modelled values (surface pressure, near-surface temperature and near-surface wind speed) are  
205 computed as the average-distance-weighted value of the four nearest continental grid points. A second selection criterion is also applied in order to reduce comparison errors due to the difference between the model surface elevation and the actual AWS elevation: we only retain observations with an elevation difference lower than 250 m. This two-stage selection leaves 41 suitable AWS in our domain (Fig. 1).

To evaluate the simulated SMB, we use airborne-radar data from Medley et al. (2013, 2014) covering  
210 the period 1980-2011. These data were collected through the NASA's Operation Icebridge campaign over the Thwaites and Pine Island basins. They are based on the CReSIS radar (Center for Remote Sensing of Ice Sheets), which is an ultra-wideband radar system able to measure the stratigraphy of the upper 20 – 30 m of the snowpack with few centimeters in vertical resolution. Airborne-radar data were verified with  
215 the simulated SMB with the 124 firn cores gathered in the GLACIOCLIM-SAMBA dataset thoroughly described by Favier et al., (2013) and updated by Wang et al., (2016).

To evaluate simulated surface melt, we use satellite-derived estimates of surface meltwater production over 1999-2009 from Trusel et al., (2013), provided at 4.45 km resolution, and based on the QuickSCAT backscatter and calibrated with in-situ observations. We also use data from Nicolas et al. (2017) who  
220 provide the number of melt days at 25 km resolution over Antarctica. This product is based on passive microwave observations from the Scanning Microwave Multichannel Radiometer (SMMR), the Special Sensor Microwave/Imager (SSM/I), and the Special Sensor Microwave Imager Sounder (SSMIS) spaceborne sensors, and covers the 1978-2017 period. For a given grid cell and a given day, melt is assumed to occur as soon as one of the two daily observations of brightness temperature exceeds a  
225 threshold value. As the identification of melt days may be sensitive to the algorithm, we also use the dataset from Picard et al. (2007), extended to 2018 (<http://pp.ige-grenoble.fr/pageperso/picardgh/melting/>, last access: 25 September 2019). This dataset is also based on SMMR and SSMI, but uses the algorithms from Torinesi et al. (2003) and Picard and Fily (2006) to retrieve melt days. It is provided as daily melt status at 25km resolution over the Antarctic continent from  
230 1979 to 2018.

### 2.3 Climate indices

To describe the ENSO, we use the Southern Oscillation Index (SOI) index from the Global Climate Observing System (GCOS) Working Group on Surface Pressure (Ropelewski and Jones, 1987; [https://www.esrl.noaa.gov/psd/gcos\\_wgsp/Timeseries/SOI/](https://www.esrl.noaa.gov/psd/gcos_wgsp/Timeseries/SOI/), last access: 25 September 2019). The SOI

Supprimé: 14 May

Supprimé: These data were collected over the Thwaites and Pine Island basins.

Supprimé: 14 May

Supprimé: El Niño

Supprimé: we use the NINO34

Supprimé: ([https://www.esrl.noaa.gov/psd/gcos\\_wgsp/Timeseries/Nino34/](https://www.esrl.noaa.gov/psd/gcos_wgsp/Timeseries/Nino34/), last access: 14 May 2019). The NINO3.4 index corresponds to SST anomalies over the 5°S-5°N and 170-120°W box (removing the 1981-2010 mean).

245 index corresponds to the normalized pressure difference between Tahiti and Darwin based on observations. The Rossby wave trains connecting the Equatorial Pacific to Antarctica are expected to develop within a few weeks in response to ENSO anomalies (e.g. Hoskins and Karoly, 1981; Mo and Higgins, 1998; Peters and Vargin, 2015), so we first use the synchronous (DJF, i.e. December-January-February) SOI index in section 3. The lagged relationship to ENSO is discussed in section 4, where we  
 250 use other 3-month averages of SOI such as JJA (June-July-August). SOI is preferred to NINO3.4 because it gives slightly stronger correlations with the variability in the Amundsen Sea region (as also found by Scott et al., 2019 and Holland et al., 2019, but very similar results were obtained using NINO3.4 (not shown).

Supprimé: NINO34

Supprimé: NINO34 such as JJA (June-July-August

We use the SAM index from NOAA/CPC (<https://stateoftheocean.osmc.noaa.gov/atm/sam.php>,  
 255 last access: 25 September 2019) to describe the primary mode of atmospheric variability in the Southern Ocean (e.g., Marshall, 2003). The SAM index is calculated as the difference of mean zonal pressure between the latitudes of 40°S and 65°S, based on NCEP-NCAR reanalysis which produces a SAM that is consistent with other reanalyses after 1979 (Gerber and Martineau, 2018). In the negative (positive) phase, the mean sea level pressure anomaly between the Antarctic and mid latitude is positive (negative) and  
 260 leads to a weaker (stronger) polar jet. Thus, positive (negative) values of the SAM index correspond to stronger (weaker)-than-average westerlies over the mid-high latitudes (50°S-70°S) and weaker (stronger) westerlies in the mid-latitudes (30°S-50°S).

Supprimé: 14 May

Supprimé: .

We use two other indices to describe the evolution of the migration and intensity variations of the Amundsen Sea Low (ASL). The datasets are provided by the British Antarctic Survey  
 265 ([https://legacy.bas.ac.uk/data/absl/ASL-index-Version2-Seasonal-ERA-Interim\\_Hosking2016.txt](https://legacy.bas.ac.uk/data/absl/ASL-index-Version2-Seasonal-ERA-Interim_Hosking2016.txt), last access: 25 September 2019), and calculated from the ERA-Interim reanalysis. To describe the migration, we use the longitudinal position of the ASL defined as the position of the minimum pressure within the box 170°-298°E, 80°-60°S (Hosking et al., 2016), defined in degree East. A decrease in the longitudinal position index hence corresponds to a westward shift of the ASL. To describe the intensity of the ASL,  
 270 we use the relative central pressure of the ASL calculated as the minimum pressure in the aforementioned box minus the average pressure over that box (Hosking et al. 2016). A more intense ASL (deeper depression) is therefore represented by a lower index.

Supprimé: 14 May

The SAM and ASL indices are defined regionally, and we do not expect any lag with summer SMB, so these indices are therefore calculated as DJF averages. All the correlations are calculated using  
 275 detrended time series.

Supprimé: . These

The correlations between these four indices are indicated in Table 1. A significant anti-correlation is obtained between the SAM index and ENSO (i.e. -SOI) as previously reported by Fogt et al. (2011). There is no significant relationship between the ASL longitudinal position and ENSO or SAM, as previously reported by Turner et al., (2013a). The relative central pressure also varies independently from SAM,  
 280 ENSO, and the ASL longitudinal position. Numerous previous studies used the absolute rather than

Supprimé: NINO34

relative central pressure to characterize the ASL, but this index is strongly correlated to the SAM index and cannot be considered independently (Table 1). As proposed by Hosking et al. (2013), the ASL relative central pressure (i.e actual central pressure minus pressure over the AS sector) allows for a better understanding of West Antarctic climate as it removes the influence of large scale variability such as ENSO and SAM.

Table 1: Correlation between climate indices  $\Delta$ SOI, SAM, ASL longitudinal position, ASL relative central pressure, ASL actual central pressure) in austral summer (December-January-February). Values in brackets represents the percentage of significance.

Statistical correlation (R)	$\Delta$ SOI	SAM	ASL Longitudinal position (°East)	ASL relative central pressure (hPa)	ASL actual central pressure (hPa)
$\Delta$ SOI		-0.45 (99%)	-0.22 (82%)	0.00 (1%)	0.40 (99%)
SAM			0.18 (73%)	-0.25 (88%)	-0.88 (99%)
ASL Longitudinal position (°East)				-0.23(84%)	-0.15 (63%)

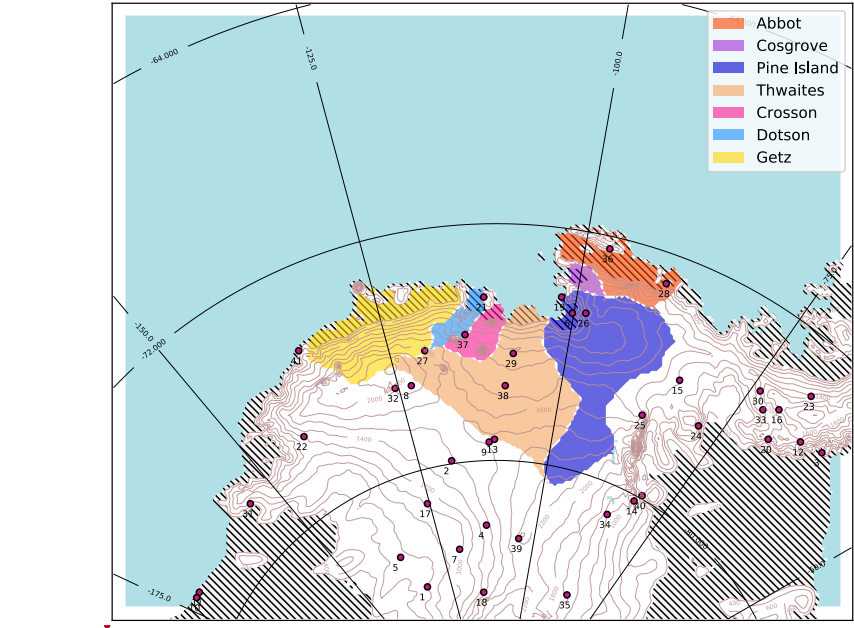


Figure 1 : Simulation domain. The drainage basins (Rignot et al., 2019) under consideration in this paper are shaded in color and Automatic Weather Station (AWS) are indicated with red point. Hatched area represents ice-shelves and contour line the surface elevation (every 200m). Station name from 1 to 41 : (1) Brianna, (2) Byrd, (3) Cape Adams, (4) Doug, (5) Elizabeth, (6) Evans Knoll, (7) Harry, (8) Janet , (9) Kominko-Slade, (10) Martha2, (11) Marthal, (12) Mount McKibben, (13) Noel, (14) Patriot Hills, (15) Siple Dome, (16) Ski Hi, (17) Swithinbank, (18) Theresa, (19) Backer Island, (20) Bean Peaks, (21) Bear Peninsula, (22) Clarke Mountains, (23) Gomez Nunatak, (24) Haag Nunatak, (25) Howard Nunatak, (26) Inman Nunatak, (27) Kohler Glacier, (28) Lepley Nunatak, (29) Lower Thwaites Glacier, (30) Lyon Nunatak, (31) Mount Paterson, (32) Mount Sidley, (33) Mount Suggs, (34) Pirrot Hills, (35) Steward Hills, (36) Thurston Island, (37) Toney Mountain, (38) Up Thwaites Glacier, (39) Whitmore Mountains, (40) Wilson Nunatak, (41) Russkaya. Relaxation zone is shown in white (~400km).



320 **3 Results**

We first evaluate the simulations with regard to observations (section 3.1). Then, we analyze the interannual variations in SMB and melting (section 3.2).

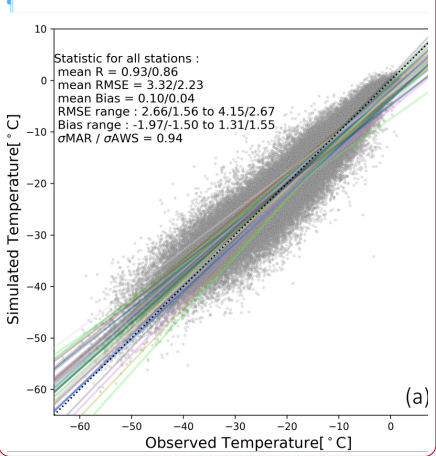
**3.1 Model evaluation**

325 We first evaluate the near-surface temperature and near-surface wind speed in comparison to AWS data (Fig.2).

Our MAR configuration reproduces the daily near-surface temperatures, with a mean bias of 0.10 °C and a mean correlation of 0.93 for the whole year and 0.86 for summer months (Fig.2a). The statistics per station show a RMSE varying from 2.66 (10<sup>th</sup> percentile) to 4.15 °C (90<sup>th</sup> percentile) and a mean bias varying from -1.97 to 1.31 °C for the whole year (see supplementary material for more details).

330 The model tends to overestimate the lowest observed wind and underestimate the highest observed  
wind speeds (regressions in Fig.2b). The model agreement with observations is nonetheless good on  
average, with a mean underestimation of 0.42 m s<sup>-1</sup>. The statistics per station show a RMSE varying from  
1.73 to 3.69 m s<sup>-1</sup>, and a mean bias varying from -3.08 to 0.85 m s<sup>-1</sup> for the whole year. The variance of  
335 the wind speed simulated by MAR is lower than observed. Less satisfactory results are generally found  
for the stations located on an island. This can be explained by the resolution of 10 km which is still too  
coarse to resolve small topographic features. For both, near-surface temperature and wind speed, the  
statistics for the summer period (December-January-February) are very similar to the statistics for the  
whole year. Our results show very similar model skills compared to other simulations in the same region  
340 (Deb et al., 2016; Lenaerts et al., 2017) or at coarser resolution over the whole ice sheet (Agosta et al.,  
2019).

**Supprimé:** The model tends to respectively overestimate and underestimate the highest and lowest observed wind speeds (regressions in Fig.2b). The model agreement with observations is nonetheless good on average, with a mean underestimation of 0.42 m s<sup>-1</sup>. The statistics per station show a RMSE varying from 1.73 to 3.69 m s<sup>-1</sup>, and a mean bias varying from -3.08 to 0.85 m s<sup>-1</sup> for the whole year. The variance of the wind speed simulated by MAR is lower than observed. Less satisfactory results are generally found for the stations located on an island. This can be explained by the resolution of 10 km which is still too coarse to resolve small topographic features. For both, near-surface temperature and wind speed, the statistics for the summer period (December-January-February) are very similar to the statistics for the whole year.



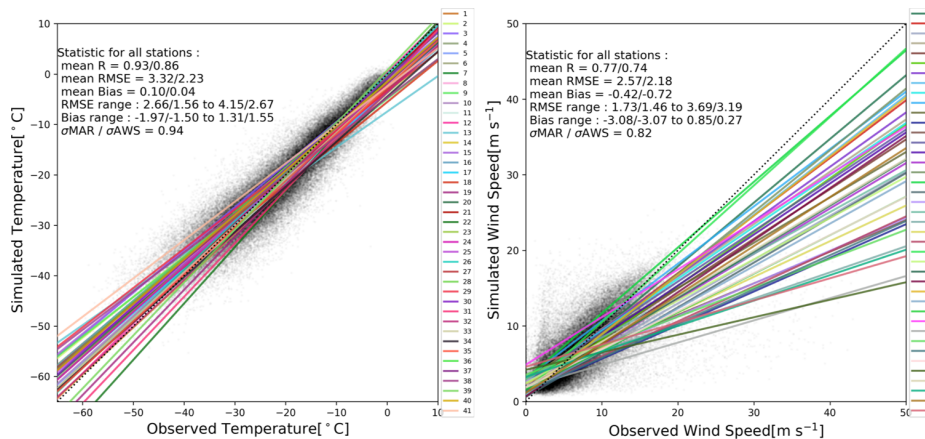


Figure 2 : Scatter plots of observed vs. simulated near-surface temperature (a) and near-surface wind speed (b) for the selected AWS (see corresponding locations and names in Fig. 1). The statistics, including Root Mean Square Error (RMSE), correlation (R), bias, and standard deviations ( $\sigma$ ), are calculated for individual stations and provided as multi-station mean over the whole year / over the summer months (December-January-February). The range of RMSE and biases across individual stations is also indicated and RMSE corresponds to the 10<sup>th</sup> percentile and the 90<sup>th</sup> percentile. The lines represent least-mean-square linear fit between simulated data and observations. The complete statistical analyses for individual AWS are provided in Supplementary material (Table S1-S2).

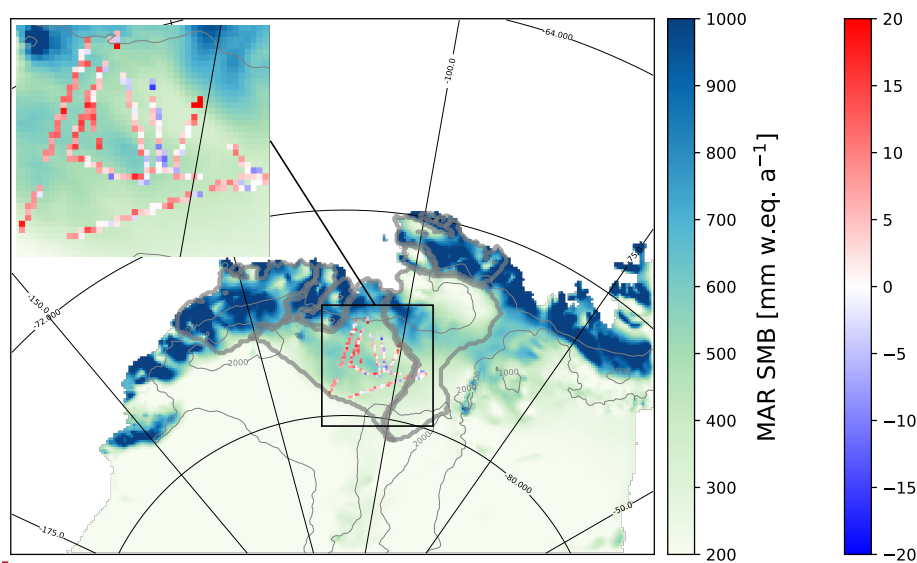
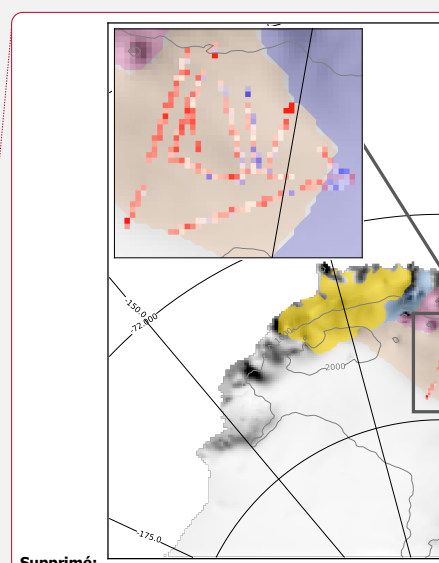


Figure 3 : Annual mean (1979-2017) simulated SMB (blue-green scale) and relative error of the simulated SMB compared to the airborne-radar data from Medley et al. (2013, 2014) (blue-red color bar). Grey contours indicate the surface height (every 1000m). The drainage basins under consideration are shaded with the same colors as in Fig.1.



Supprimé:

Supprimé: grey

We now assess the simulated SMB compared to the SMB from Medley et al., (2013, 2014) derived from airborne radar over the period 1980-2011. The simulated SMB is well captured by MAR with a mean relative overestimation of approximately 10% over the Thwaites basin, and local errors smaller than 20% at all locations (Fig.3). The interannual variability is also well simulated by MAR with a correlation of 0.90 (Fig.4). In order to have a broad overview of the SMB evaluation, we also compared the simulated SMB with the GLACIOCLIM-SAMBA dataset (Favier et al., 2013) over the Ross and Siple Coast sector (See Fig.S1 in Supplementary material). The bias of simulated SMB compared to observation is less than 10 mm w.e a<sup>-1</sup> and local bias can reach 30 mm w.e a<sup>-1</sup>. However, the relative bias between GLACIOCLIM-SAMBA dataset and simulated SMB is more pronounced with only 44% of GLACIOCLIM-SAMBA sites show a relative error with simulated SMB lower than 20%.

Supprimé: (Medley et al. 2013, 2014).

Supprimé:

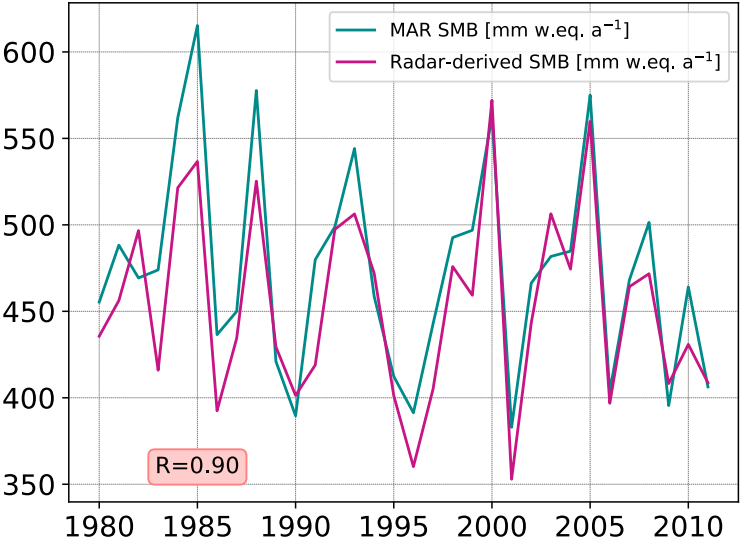


Figure 4 : Timeseries of the annual mean (January to December) simulated and radar-derived SMB from 1980 to 2011 over the Thwaites basins.

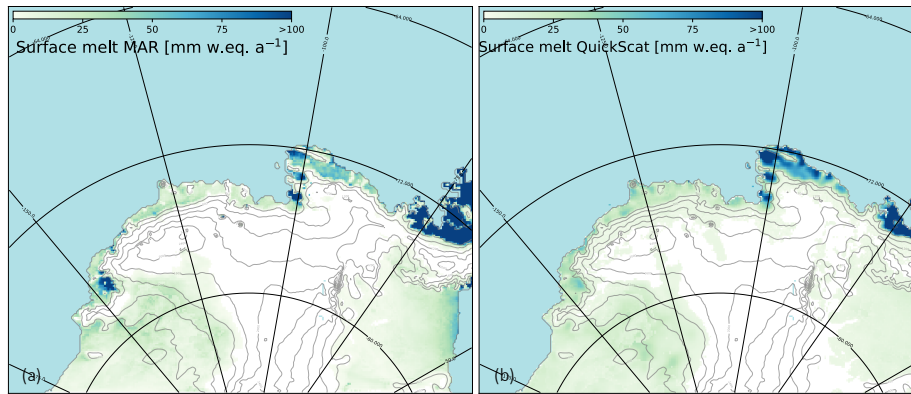
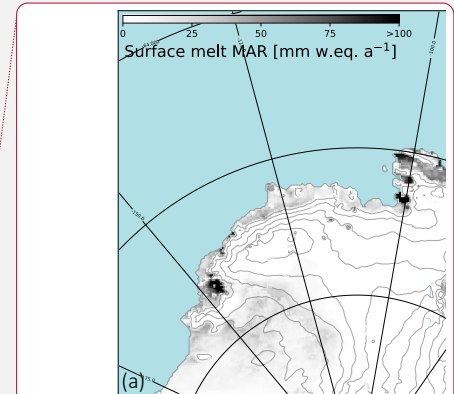


Figure 5 : Annual surface melt rate (a) simulated by MAR over 1999-2009, and (b) derived from QuickScat satellite data over the same period (Trusel et al. 2013) and interpolated over the MAR grid.



Supprimé:

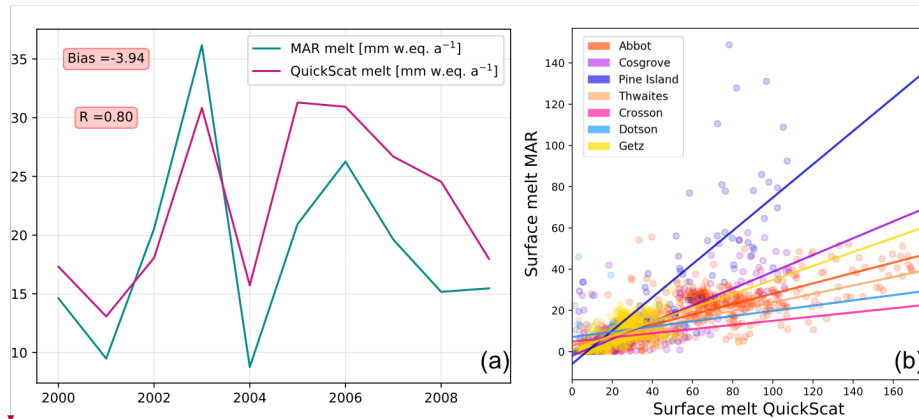
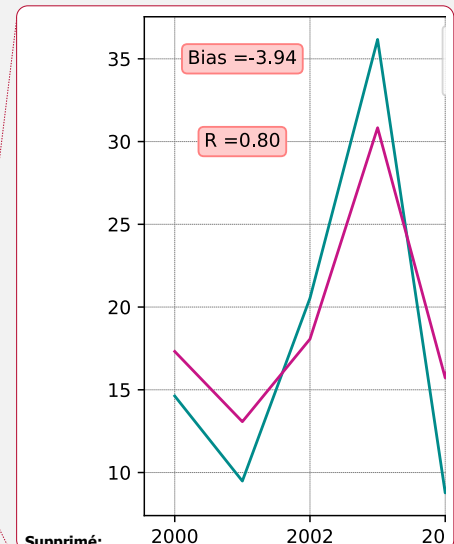


Figure 6 : (a) Time series of surface melt rates in mean over the model domain derived from satellite data and simulated by MAR, years labelled on the X-axis refer to the second year of a given austral summer (e.g., summer 1999-2000 is labelled 2000), and (b) Surface melt modelled versus surface melt interpolated from satellite data (QuickScat) over drainage basins, (only where surface melt > 0 mm w.e. a⁻¹) and over the period 1999-2009.



Supprimé:

Supprimé: (only where surface melt > 0 mm w.e. a⁻¹) and over the period 1999-2009,

Supprimé: . Years

The areas of highest surface melt ( $> 100 \text{ mm w.e. a}^{-1}$ ) are located near the coast and particularly over Abbot, Cosgrove, and the eastern part of Pine Island ice shelf, while more extreme values ( $> 200 \text{ mm w.e. a}^{-1}$ ) are found near the Peninsula in both simulated and observed datasets (Fig. 5). Even if the simulated and observed patterns are similar, the simulated surface melt is a factor of two lower than observations locally (e.g. over Abbot ice shelf and the Peninsula). While the interannual melt rate variability is well reproduced with a correlation of 0.80, the surface melt rate simulated by MAR is underestimated by 18% on average compared to QuickScat estimates (Fig. 6a). Surface melt rate over Pine Island basins is well simulated by MAR (Fig. 6b) with R equal to 0.80 compared to drainage basins with low surface melt (i.e. Crosson, Dotson) where R is equal to 0.14 and 0.24 respectively. This melt underestimation, particularly

Supprimé: 6). This melt underestimation

pronounce over drainage basins with low surface melt rate, could be explained by the slight overestimation of the snowfall accumulation (10-20%), as the presence of a fresh snow layer of high albedo overlying snow or ice layers of lower albedo likely reduces melt. MAR presents slight overestimation over Getz ice-shelf (Fig.5) possibly explained by wind advection, föhn effect, or even snow metamorphism simulated by MAR. Further work is needed to understand such local biases. MAR is fully driven by low resolution ERA-Interim sea ice cover and temperature therefore possible underestimation of the presence of polynyas can also play a role in the melt biases.

Supprimé: underestimation.

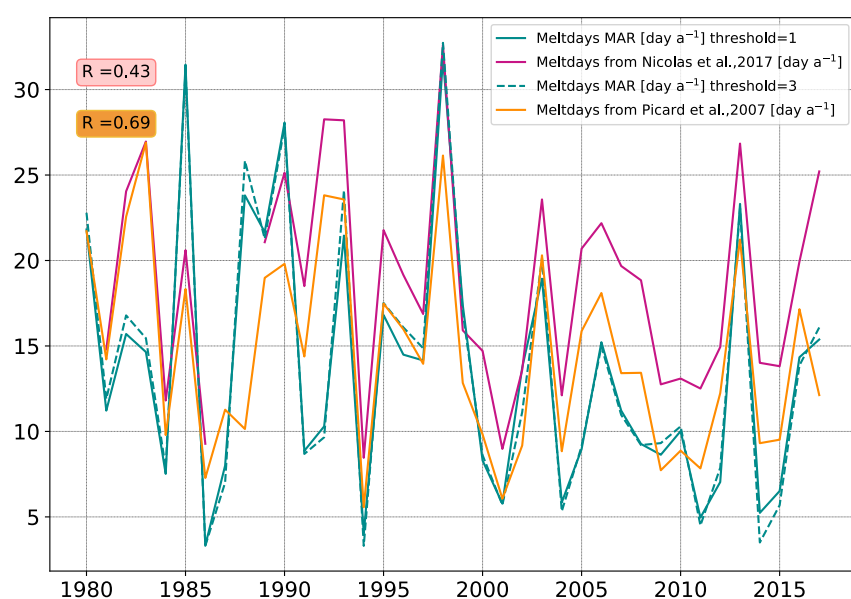


Figure 7 : Time series of number of melt days per summer (DJF) averaged over the part of the domain with more than 3 melt days per year on average (which approximately corresponds to the ice shelf zone), derived from two satellite products and simulated by MAR (defined using a melt-rate threshold of either 1 or 3 mm w.e.day<sup>-1</sup>).

We also compare the number of melt days to the satellite products from Nicolas et al. (2017) and Picard et al. (2007). To avoid no melt days area in the timeseries computation we use the area where annual number of melt days for each dataset is more than 3 melt days per year, that corresponds approximately to the ice shelf zone. As with the amount of surface melt, the number of melt days over the domain is underestimated by MAR (Fig.7). The amplitude of the underestimation is not very sensitive to the melt-rate threshold used to define a melt day in MAR. A threshold of 1 mm w.e. day<sup>-1</sup> (as in Datta et al., 2019) gives a mean underestimation of 4.8 days per year compared to observation from Nicolas et al. (2017), while a threshold 3 mm w.e. day<sup>-1</sup> (as in Deb et al., 2018; Lenaerts et al., 2017) gives a mean

Supprimé: 1mm

underestimation of 4.9 days per year. This underestimation is less pronounced (0.8 to 0.9 day per year depending on the threshold) when using Picard et al. (2007) as a reference. The interannual variability in the number of melt days is reproduced with correlations of 0.69 and 0.43 to the two satellite products (Fig. 7). Previous study on Antarctic Peninsula also found that MAR melt occurrence is comparable to satellite products, but slightly underestimated over the Western coast of the Peninsula (Datta et al., 2019).

Overall, MAR well simulates the interannual variability of the Amundsen sector, and we are now going to use these simulations to investigate the drivers of interannual variability of SMB and surface melting.

### 3.2 Drivers of summer interannual variability

In this subsection, we first investigate the large-scale conditions leading to interannual anomalies in summer SMB or surface melting. For a sake of clarity, we only consider the Pine Island and Thwaites basin (together) as a first approach. To identify large-scale conditions leading to high (low) SMB, we calculate composites defined as the average of summers presenting a SMB greater than the 85<sup>th</sup> (lower than the 15<sup>th</sup>) interannual percentile, and we proceed similarly for surface melt composites. We choose the 85<sup>th</sup> and 15<sup>th</sup> percentiles to optimize the signal-to-noise ratio.

Supprimé: (DJF means)

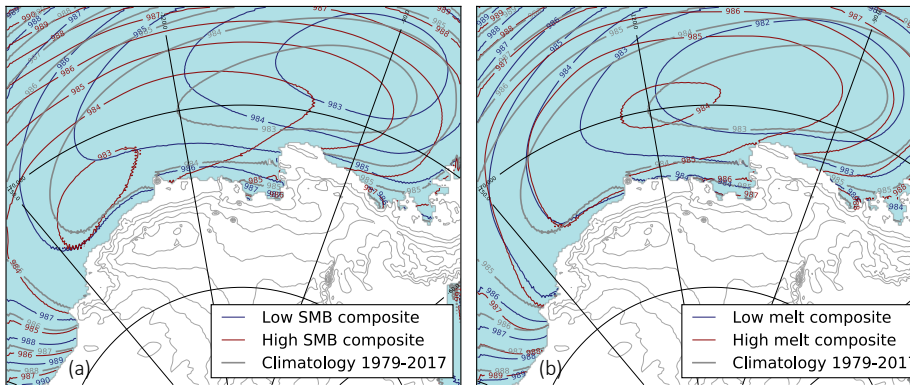


Figure 8 : Summer sea surface pressure composites for high/low SMB (a) and high/low surface melt (b). The ice-sheet height is indicated by thin grey contours (every 500m).

Sea surface pressure composites show that distinct mechanisms affect the interannual variability of summer SMB and surface melting (Fig. 8). Summers with high SMB are on average characterized by a far westward (by  $\sim 30^\circ$ ) and southward (by  $3-4^\circ$ ) migration of the ASL center, while the reverse migration is found for summers with low SMB although with a smaller displacement ( $\sim 15^\circ$  eastward). In contrast, years with high surface melt rates are characterized with a much smaller ASL migration and no migration

475 is found for years with low surface melt rates, but the pressure gradients differ between the high and low composites. Therefore, we hereafter consider the variability of SMB and surface melting separately.

On average, low-SMB summers are characterized by a northward and eastward ASL migration (shown through a dipole in the 500hPa normalized geopotential composite in Fig. 9a,c), which is associated with an offshore surface wind anomaly over the glaciers of the Amundsen sector (Fig. 9e). Conversely, high-SMB summers are characterized by a southward and westward ASL migration (Fig. 9b,d), which is associated with an onshore surface wind anomaly over the glaciers of the Amundsen sector (Fig. 9f). The circulation anomalies typical of high-SMB summers favor the southward transport of precipitable water, as indicated by the composites of integrated vapor transport (Fig. 10a,b). Increased moisture transport towards the Amundsen Sea Embayment leads to denser cloud cover (Fig. 10c,d) and increased SMB.

On average, high-melt summers are also associated with increased moisture transport towards the Amundsen Sea Embayment, and conversely for low-melt summers (Fig. 11a,b), but the mechanism is somewhat different from the case of SMB. The ASL migration during high-melt summers is much smaller than for the high-SMB summers (Fig. 8b). Summers with high surface melt rates show a significant increase in the 500 hPa geopotential height over the Bellingshausen Sea (Fig. 12b), i.e. an anticyclonic anomaly, and small westward ASL migration as shown in the 500hPa normalized geopotential composite (Fig. 12d). This anomaly is against the ASL mean circulation and creates a northerly flow anomaly over the ice sheet in the Amundsen sector (Fig. 12e,f). This anticyclonic anomaly was described by Scott et al. (2019) in terms of enhanced blocking activity. As in Scott et al. (2019), we find that high-melt summers are associated with denser cloud cover (Fig. 11c,d), increased downward longwave radiation (Fig. 11e,f), and therefore surface air warming, while the opposite occurs for low-melt summers. Composites of sensible heat flux indicate that heat is lost by the snow surface to the atmosphere for high-melt summers, i.e. high melt summers are not caused by föhn events on average (Fig. S2).

500 Table 2 : Annual surface mass balance decomposition for all drainage basins over 1979-2017 with SMB = Snowfall + Rainfall – Sublimation – Runoff

SMB composant [ mm w.e. a <sup>-1</sup> ]	Abbot	Cosgrove	Pine Island	Thwaites	Crosson	Dotson	Getz
Surface Mass balance	959.5	660.5	429.4	504.5	867.7	895.0	843.0
Sublimation	26.5	30.3	12.7	0.6	22.6	25.6	22.8
Snowfall	981.9	688.5	441.3	505.0	887.6	919.5	864.9
Rainfall	4.0	2.3	0.4	0.1	2.8	1.1	0.8
Runoff	0.0	0.0	0.0	0.0	0.0	0.0	0.0
Refreezing	36.4	27.0	4.3	1.0	6.2	7.2	9.6
Surface melt	32.5	24.8	3.9	0.9	3.4	6.1	8.8

Supprimé: In the following...herefore, we therefore ... [1]

Supprimé: 700hPa...00hPa normalized geopotential composite in Fig. 9a,c), which is associated with an offshore surface wind anomaly [2]

Supprimé: convergence...ransport towards the Amundsen Sea... [3]

Supprimé: [4]

Déplacé vers le bas [1]: Anomalies are calculated as high/low

Déplacé vers le bas [2]: and (c,d) cloud cover (no units, from

Supprimé: [5]

Supprimé: OLD [6]

Supprimé: OLD [7]

Supprimé: 45

Supprimé: 48

Supprimé: 07

Supprimé: 51

Supprimé: 72

Supprimé: 04

Supprimé: 842.98

Supprimé: 47

Supprimé: 32

Supprimé: 67

Supprimé: 62

Supprimé: 64

Supprimé: 63

Supprimé: 79

Supprimé: 93

Supprimé: 53

Supprimé: 32

Supprimé: 55

Supprimé: 54

Supprimé: 93

Supprimé: 3.99

Supprimé: 27

Supprimé: 42

Supprimé: 14

Supprimé: 81

Supprimé: 13

Supprimé: 84

Supprimé: 44

Supprimé: 03

Supprimé: 34

Supprimé: 04

Supprimé: 20

Supprimé: 24

Supprimé: 61

Supprimé: 45

Supprimé: 76

Supprimé: 92

Supprimé: 91

Supprimé: 39

Supprimé: 11

Supprimé: 77



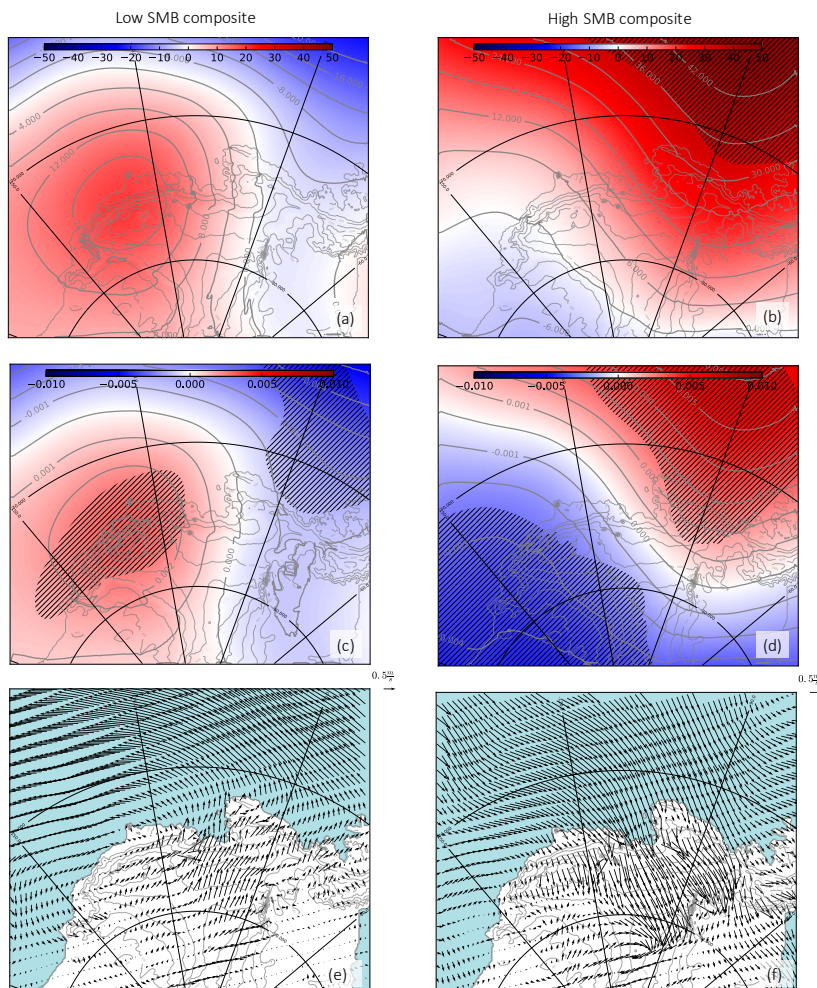
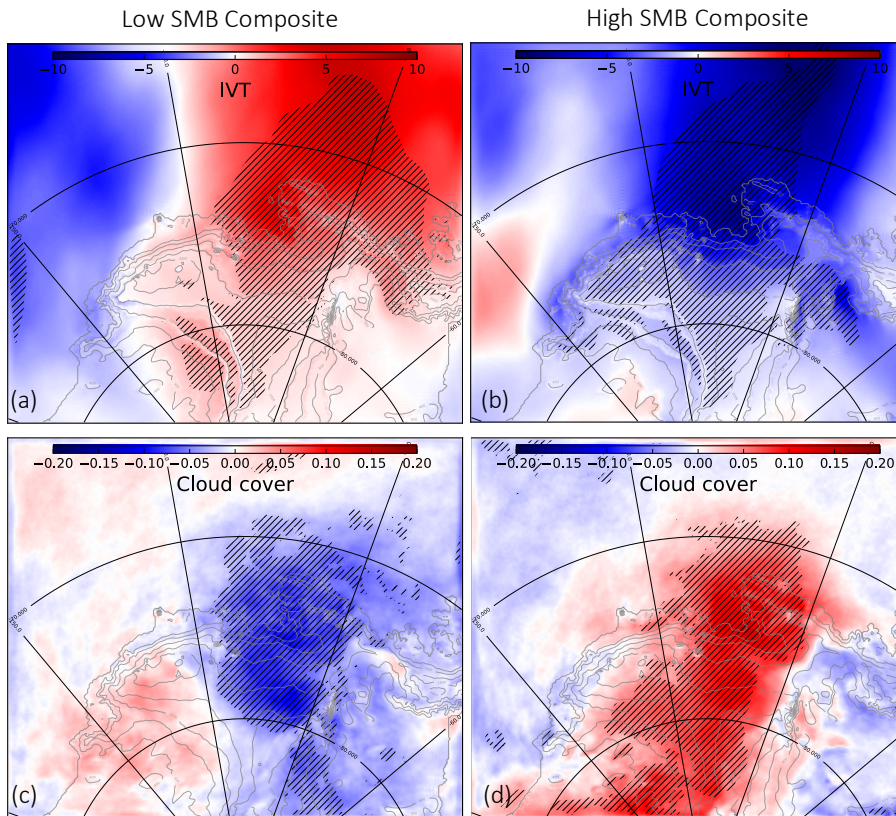


Figure 9 : (a,b) 500 hPa geopotential height (m), (c,d) 500 hPa geopotential height divided by the domain-averaged value for each season and (e,f) 10m wind ( $\text{m s}^{-1}$ ) anomalies during low-SMB summers (left) and high-SMB summers (right). Anomalies are calculated as high/low composites minus the climatology over 1979-2017. Hatched area represents significance >90% calculated with a *t*-test.

Déplacé (insertion) [1]

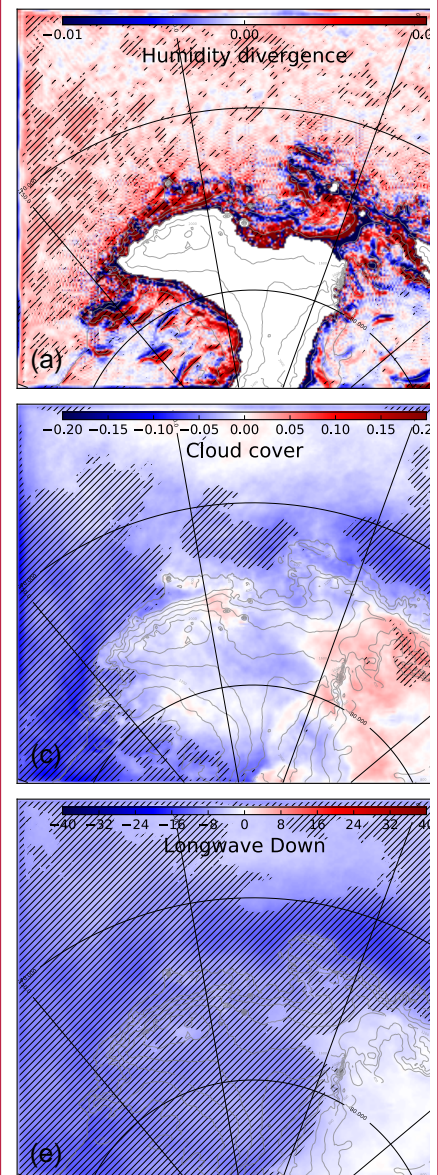


**Figure 10:** (a,b) vertical Integrated Vapor Transport (IVT) along the y-axis ( $\text{kg m}^{-2}$ , negative toward the continent) calculated as  $IVT = \int_{925}^{700} q \cdot v \frac{dp}{g}$  and (c,d) cloud cover (no units, from 0 to 1) anomalies during low-SMB summers (left) and high-SMB summers (right). Anomalies are calculated as high/low composites minus the climatology over 1979–2017. Hatched area represents significance > 90% calculated with a *t*-test.

Déplacé (insertion) [2]

Supprimé: Saut de page

Low surface melt composite





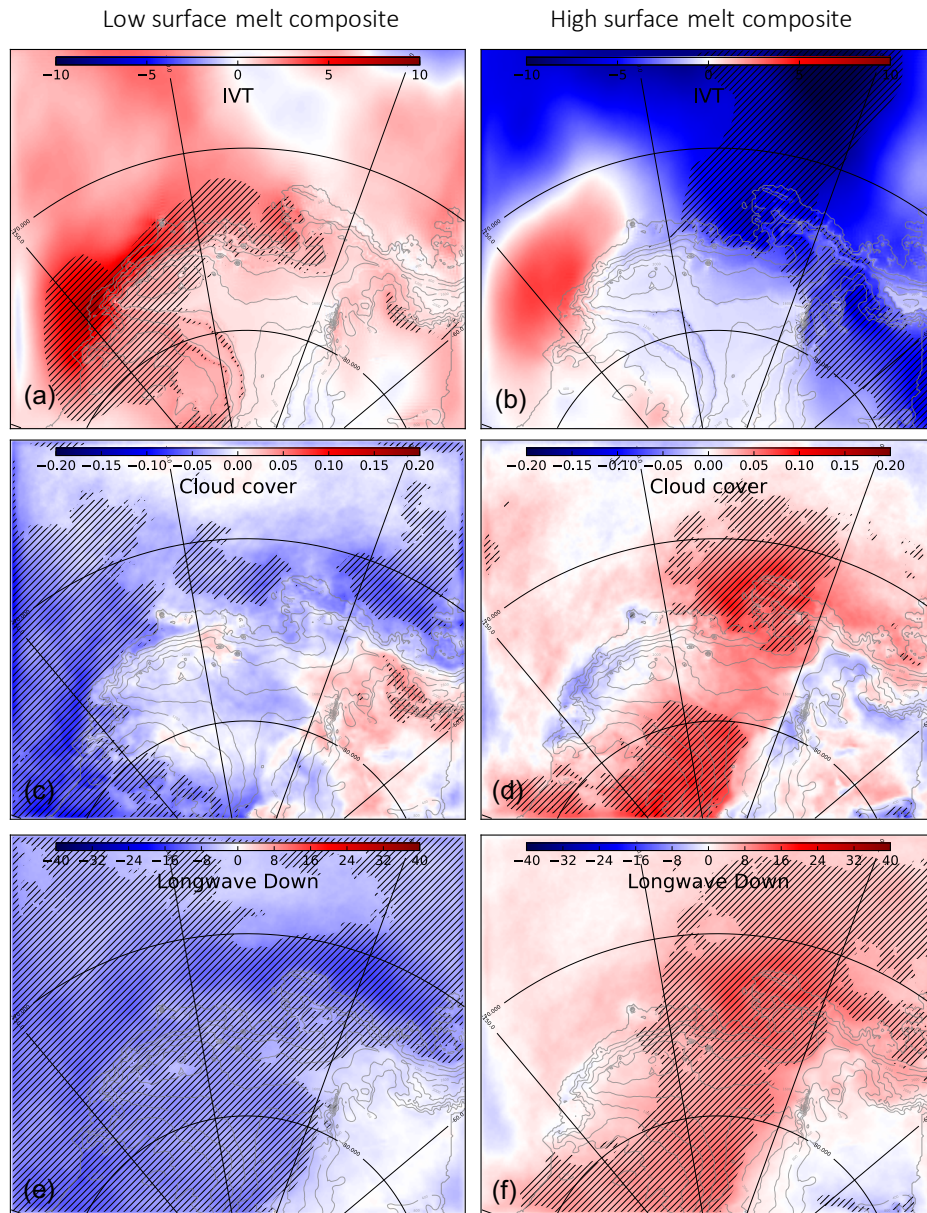


Figure 11 : (a,b) **vertical Integrated Vapor Transport (IVT) along y axis (negative toward the continent) ( $\text{kg m}^{-2}$ ) (same formula as for SMB)**, (c,d) cloud cover (no units, from 0 to 1), and (e,f) downward longwave radiation ( $\text{W m}^{-2}$ ) anomalies during low-melt summers (left) and high-melt summers (right). Anomalies are calculated as high/low composites minus the climatology over 1979-2017. Hatched area represents significance > 90% calculated with a *t*-test.

Supprimé: humidity divergence at 850 hPa ( $\text{g kg}^{-1} \text{s}^{-1}$ )

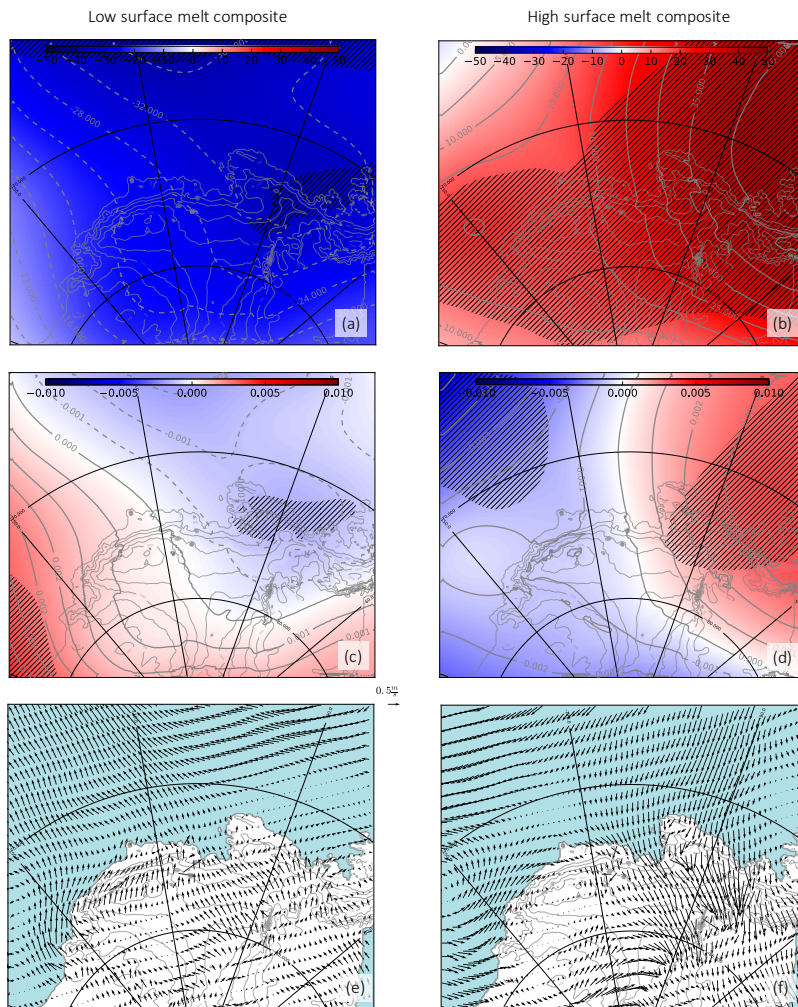
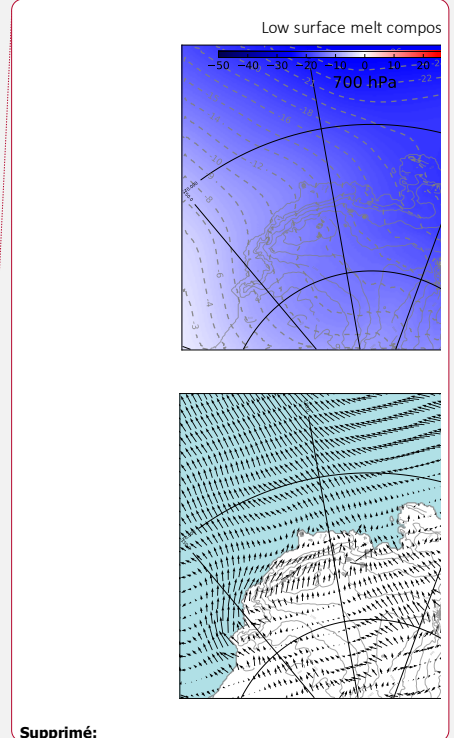


Figure 12 : (a,b) 500 hPa geopotential height (m) and (c,d) 500 hPa geopotential height divided by the domain-averaged value for each season and (e,f) 10m wind ( $\text{m s}^{-1}$ ) anomalies during low-melt summers (left) and high-melt summers (right). Anomalies are calculated as high/low composites minus the climatology over 1979-2017. Hatched area represents significance >90% calculated with a *t*-test.



Supprimé:

Supprimé: 700

Supprimé: that

Supprimé: in

Now that we have described the mechanisms in play for summers with high and low SMB or surface melt rates, we investigate the connections between the leading modes of climate variability (ENSO, SAM and ASL variability) and summer SMB and surface melting over the individual Amundsen drainage basins (shown in Fig.1).

In line with the previous composite analysis for high and low SMB composites, the SMB in all the drainage basins is anti-correlated to the ASL longitudinal position (Table 3, 4<sup>th</sup> column). This anti-

correlation has little statistical significance for Abbot and Cosgrove, but for Dotson and Thwaites, the ASL longitudinal position explains nearly 40% of the SMB interannual variance (explained variance given by square correlations). The ENSO-SMB relationship has moderate levels of statistical significance, with positive SMB correlations to  $\sqrt{\text{SOI}}$  for all basins, but a part of SMB variance explained by ENSO that remains below 16% (Table 3, 2<sup>nd</sup> column).  $\sqrt{\text{SOI}}$  and the ASL longitudinal location are not significantly connected together (Table 1), therefore their connection to SMB can be considered as independent from each other. Finally, the SMB is significantly correlated to neither the ASL relative central pressure (Table 3, 5<sup>th</sup> row) nor the SAM index (Table 3, 3<sup>rd</sup> column) for all the basins. To better describe interplays, we also calculate a multi-linear regression of SMB on the 4 indices (last column of Tab. 3). Accounting for several indices increases the explained SMB variance compared to a single index, indicating an interplay of the ASL and ENSO. Overall, 16 to 49% of the summer SMB variance (increasing westward) can be explained by a linear combination of the climate indices.

**Table 3 : Correlation R between ENSO, SAM, and ASL indices and the SMB over individual drainage basins in austral summer. The statistical significance (t-test) is written within brackets. The last column shows the correlation of a multi-linear regression to the 4 indices using a least absolute shrinkage and selection operator (LASSO, Tibshirani, 1996)**

Drainage Basins	-SOI vs SMB	SAM index vs SMB	ASL longitudinal location vs SMB	ASL relative central pressure vs SMB	multi-linear regression
Abbot	0.25 (87%)	0.14 (59%)	-0.15 (65%)	-0.01 (3%)	0.40
Cosgrove	0.26 (88%)	0.16 (65%)	-0.21(80%)	0.08 (36%)	0.46
Pine Island	0.32 (95%)	0.03 (17%)	-0.25 (87%)	-0.17 (69%)	0.47
Thwaites	0.33 (96%)	0.02 (8%)	-0.45 (99%)	-0.10 (47%)	0.57
Crosson	0.40 (99%)	-0.00 (2%)	-0.53 (99%)	-0.14 (60%)	0.66
Dotson	0.36 (97%)	0.00 (2%)	-0.61 (99%)	0.15 (65%)	0.70
Getz	0.30 (93%)	-0.15 (62%)	-0.64 (99%)	0.27 (90%)	0.68

We now investigate similar relationships, but with surface melt rates instead of SMB. By contrast to SMB, the surface melt connection to the ASL relative central pressure is stronger than its connection to the ASL longitudinal position (Table 4, 4<sup>th</sup> and 5<sup>th</sup> columns), which again highlights the two distinct mechanisms explaining high/low melt rates vs high/low SMB. The part of the melt rate variance explained by the ASL relative central pressure increases westward, from 12% for Abbot to 21% for Getz. Even though the effect of the ASL central pressure dominates, there is still a moderate anti-correlation between melt rates and the ASL longitudinal position, suggesting that the mechanism explaining high/low SMB can explain a small part of the melt rate variance (less than 10%). In a similar way as SMB,  $\sqrt{\text{SOI}}$  explains

Supprimé: NINO34

Supprimé: 10

Supprimé: NINO34

Déplacé vers le bas [3]: central pressure (Table 3, 5<sup>th</sup> row) nor the SAM index (Table 3, 3<sup>rd</sup> column) for all the basins.

Déplacé (insertion) [3]

Supprimé: ¶

Supprimé: Drainage Basins

... [8]

Supprimé: As in the case of

Supprimé: NINO34

less than 9% of the melt rate's variance, with moderate statistical significance (Table 4, 2<sup>nd</sup> column), and as for summer SMB there is no significant relationship to the SAM. We have repeated the calculations considering the number of melt days, and we find very similar results in terms of correlations (Table 4, 2<sup>nd</sup> line in each row). Relatively similar conclusions can be drawn from observational estimates of number of melt days (values in italic in Table 4), except that satellite estimates indicate a stronger correlation to -SOI, even exceeding the correlation to the ASL central pressure in the case for most drainage basins (the variance explained by -SOI reaching 25%). As the SAM index is significantly anti-correlated to ENSO (Table 1), the stronger melt-SOI correlation in the observational products goes together with a stronger melt-SAM anti-correlation than in our simulations. To better describe interplays, we also calculate a multi-linear regression of melt rates on the 4 indices (last column of Tab. 4). Accounting for several indices increases the explained melt rate variance compared to a single index, which indicates an interplay of the four modes of variability. Overall, 21 to 30% of the summer melt rate variance can be explained by a linear combination of the climate indices.

The part of explained variance never exceeds 50% of the summer melt and SMB variance. Possible reasons for this are (i) the modes of variability do not explain all the variance locally; for example, the leading EOF of SST in the Equatorial Pacific (representing ENSO) only accounts for 50 to 70% of the SST variance (e.g. Roundy, 2014) meaning that the tropical convection thought to influence Antarctica is not completely described by SOI or NINO3.4; (ii) assuming that a large part of the tropospheric circulation variability is explained by ENSO, SAM and ASL indices, there are reasons why the connection may be weaker for SMB and surface melting because of their non-linear dependence on sea ice and evaporation in coastal regions, the evolution of snow properties, etc; (iii) strong modulation of the southeast Pacific extratropical circulation by Rossby wave train is not only due to the existence of El Niño events but also depends on the exact spatial distribution of deep convection in the tropical central Pacific and to the strength of the polar jet (Harangozo, 2004) (iv) a part of the variability of SMB and melting may be stochastic, i.e. not necessarily driven by variability with spatio-temporal coherence at large scales.

Supprimé: 10

Supprimé: rates

Supprimé: instead of melt rates

Supprimé: NINO34

Supprimé: of Pine Island and Thwaites

Supprimé: NINO34

Supprimé: NINO34

Supprimé: ¶  
.....Saut de page.....



Table 4 : Correlation R between  $\downarrow$ SOI, SAM, and ASL indices and MAR surface melt rates (bold), MAR number of melt days (regular), number of melt days from satellite products (italic, first value for Nicolas et al. (2017) and second for Picard et al. (2007), over individual ice-shelves in summer. The statistical significance (t-test) is written within brackets. **The last column shows the correlation of a multi-linear regression to the 4 indices using a least absolute shrinkage and selection operator (LASSO, Tibshirani 1996).**

Drainage Basins	$\downarrow$ SOI	SAM index	ASL longitudinal location	ASL relative central pressure	multi-linear regression
Abbot	<b>0.23 (84%)</b>	<b>-0.05 (24%)</b>	<b>-0.25 (86%)</b>	<b>0.35 (97%)</b>	<b>0.46</b>
	0.25 (86%)	-0.04 (19%)	-0.23 (84%)	0.30 (93%)	0.44
	0.37 (97%)	-0.22 (79%)	-0.29 (91%)	0.32 (94%)	0.49
	0.27 (98%)	-0.18 (71%)	-0.18 (72%)	-0.24 (92%)	0.47
Cosgrove	<b>0.24 (86%)</b>	<b>-0.08 (36%)</b>	<b>-0.30 (93%)</b>	<b>0.37 (98%)</b>	<b>0.50</b>
	0.25 (87%)	-0.06 (29%)	-0.29 (92%)	0.32 (95%)	0.47
	0.37 (97%)	-0.20 (76%)	-0.37 (97%)	0.32 (94%)	0.52
	0.38 (98%)	-0.25 (87%)	-0.16 (65%)	0.27 (90%)	0.46
Pine Island	<b>0.30 (86%)</b>	<b>-0.07 (33%)</b>	<b>-0.31 (94%)</b>	<b>0.38 (98%)</b>	<b>0.54</b>
	0.29 (92%)	-0.03 (13%)	-0.34 (96%)	0.35 (97%)	0.55
	0.48 (99%)	-0.29 (91%)	-0.21 (78%)	0.42 (99%)	0.62
	0.44 (99%)	-0.19 (75%)	-0.13 (56%)	0.37 (98%)	0.59
Thwaites	<b>0.29 (92%)</b>	<b>-0.13 (56%)</b>	<b>-0.25 (87%)</b>	<b>0.39 (98%)</b>	<b>0.51</b>
	0.35 (95%)	-0.11 (43%)	-0.19 (69%)	0.51 (99%)	0.67
	0.48 (99%)	-0.23 (81%)	-0.11 (45%)	0.29 (91%)	0.55
	0.44 (99%)	-0.28 (89%)	-0.06 (26%)	0.26 (87%)	0.52
Crosson	<b>0.28 (91%)</b>	<b>-0.14 (60%)</b>	<b>-0.23 (84%)</b>	<b>0.41 (99%)</b>	<b>0.51</b>
	0.29 (86%)	-0.08 (30%)	-0.11 (42%)	0.40 (97%)	0.52
	0.48 (99%)	-0.35 (95%)	-0.20 (76%)	0.39 (98%)	0.61
	0.35 (96%)	-0.35 (96%)	-0.10 (45%)	0.41 (98%)	0.52
Dotson	<b>0.27 (90%)</b>	<b>-0.14 (60%)</b>	<b>-0.24 (86%)</b>	<b>0.42 (99%)</b>	<b>0.52</b>
	0.26 (86%)	-0.13 (54%)	-0.25 (86%)	0.44 (99%)	0.53
	0.36 (95%)	-0.27 (84%)	-0.03 (11%)	0.36 (94%)	0.52
	0.33 (93%)	-0.28 (86%)	0.13 (51%)	0.32 (91%)	0.50
Getz	<b>0.22 (82%)</b>	<b>-0.16 (65%)</b>	<b>-0.26 (88%)</b>	<b>0.46 (99%)</b>	<b>0.53</b>
	0.22 (82%)	-0.16 (67%)	-0.29 (92%)	0.46 (99%)	0.54
	0.50 (99%)	-0.42 (99%)	-0.24 (84%)	0.41 (99%)	0.64
	0.34 (96%)	-0.41 (98%)	-0.15 (63%)	0.34 (96%)	0.46

Supprimé: NINO34

Supprimé: NINO34

Supprimé: 17 (70)

Supprimé: 18 (72)

Supprimé: 32 (94)

Supprimé: 30 (94)

Supprimé: 21 (79)

Supprimé: 19 (75)

Supprimé: 34 (95)

Supprimé: 33 (96)

Supprimé: 28 (91)

Supprimé: 26 (89)

Supprimé: 47

Supprimé: 47

Supprimé: 24 (85)

Supprimé: 27 (87)

Supprimé: 50

Supprimé: 46

Supprimé: 26 (88)

Supprimé: 18 (65)

Supprimé: 44

Supprimé: 33 (95)

Supprimé: 89

Supprimé: 0.24 (84%)

Supprimé: 31 (90)

Supprimé: 30 (89)

Supprimé: 81

Supprimé: 20 (77)

Supprimé: 42

Supprimé: 28 (91)



#### 4 Discussion

845 The composite analysis and the correlation of SMB and melt rates to the ASL indices gives a consistent picture. Summers tend to be associated with high SMB when the ASL migrates westward and southward because this places the northerly flow (ASL eastern flank) over the Amundsen Sea, thereby increasing the southward humidity transport and snowfall. This corresponds to the large-scale features described by Hosking et al. (2013) but is here described for the SMB of individual drainage basins. By contrast, longitudinal migrations of the ASL are not the main driver of surface melting variability, as previously noted by Deb et al. (2018). Summers tend to be associated with high surface melt rates when the Amundsen/Bellingshausen region experiences blocking, i.e. anticyclonic conditions, which tends to decrease the climatological southerly flow (western flank of the ASL), and to favor marine air intrusions that make cloud cover denser with increase downward longwave radiation, as described by Scott et al. (2019).

855 While the role of the ASL now appears to be quite clear, the exact impact of ENSO on SMB and surface melt rates remains elusive. Earlier studies analyzing the impact of ENSO on precipitation in West Antarctica had difficulties understanding the mechanisms and the robustness of the signal, because they had to rely on relatively short observation and reanalysis periods (Bromwich et al., 2000; Cullather et al., 1996; Genthon and Cosme, 2003). Using a dedicated SMB model over a longer time period, we have shown here that the ENSO-SMB relationship in austral summer exists, but it is relatively weak as SOI alone cannot explain more than 16% of the interannual variance in summer SMB. The relationship between ENSO and the number of melt days was identified by Deb et al. (2018) using both regional simulations and a satellite product. It was then thoroughly described by Scott et al. (2019) who found that SOI could explain 20% of the melt variance when considering all the Amundsen ice shelves together and using satellite products (correlation of 0.45 in their Table 3). While we obtain similar results as Scott et al. (2019) when using the number of melt days derived from satellite products, both the number of melt days and the melt rates simulated by MAR indicate less variance explained by SOI, that is, between 5% and 9% for the individual drainage basins. Our MAR simulations certainly contain biases in the representation of the melting process and the way it affects surface properties such as albedo and roughness, but it is also possible that the number of melt days derived from microwave satellite data is biased due to variability in surface conditions, percolation within fresh snow, meltwater ponding (observed on Pine Island, Kingslake et al., 2017), and satellite overpass time (Tedesco, 2009 ; Scott et al., 2019). More work will be needed to understand these differences.

875 Numerous publications have explained the remote effects of ENSO on the West Antarctic climate through Rossby wave trains that connect the convective anomalies associated with ENSO in the equatorial Pacific to Antarctica (e.g., Yuan and Martinson, 2001). However, austral winter and spring conditions are more favorable for Rossby wave trains to be formed and to propagate to high southern latitudes than summer conditions (Harangozo, 2004; Lachlan-Cope and Connolley, 2006; Ding et al., 2011 and

**Déplacé vers le bas [4]:** Summers tend to be associated with high surface melt rates when the Amundsen/Bellingshausen region experiences blocking, i.e. anticyclonic conditions, which tends to decrease the climatological southerly flow (western flank of the ASL), and to favor marine air intrusions that make cloud cover denser

**Supprimé:** and increase downward longwave radiation. In terms of SMB-ASL relationship, this

**Déplacé (insertion) [4]**

**Supprimé:** to understand

**Supprimé:** NINO34

**Supprimé:** 8

**Supprimé:** summer melting

**Supprimé:** NINO34

**Supprimé:** 18

**Supprimé:** 42

**Supprimé:** NINO34

**Supprimé:** 3

**Supprimé:** 8

**Supprimé:** However, Ding et al. (2011) found little connection between equatorial convection and Antarctica through Rossby wave trains in DJF, as opposed to previous MAM and JJA. This result

900 references therein). The poleward propagation of tropically sourced Rossby waves in summer is indeed inhibited by the strong polar front jet in the South Pacific sector at that time of the year, which leads to Rossby wave reflection away from the Amundsen Sea region (Scott Yiu and Maycock, 2019). This lack of direct connection in summer was supported by Steig et al. (2012) who found weakest correlations between NINO3.4 and wind stress anomalies in the Amundsen Sea in DJF compared to other seasons.

905 Therefore, we investigated possible lags in the relationships to ENSO. While ENSO peaks in DJF, it starts to develop in MAM, as indicated by the growing SOI auto-correlation from 9 to 6 months lag (Fig. 13a). The first implication of this is that any signal correlated to SOI in DJF will be correlated to SOI in the previous JJA without the need for a lagged physical mechanism. Nevertheless, the correlation between SMB or melt rates in DJF and SOI in the preceding JJA is higher than the synchronous correlation for all

910 the drainage basins (solid curves in Fig. 13b-h), which suggests that the lagged relationship is not only a simple statistical artifact. The results of Ding et al. (2011) and Steig et al. (2012) suggest that there could be a lagged mechanism whereby ENSO would influence West Antarctica in austral spring or winter, with a delayed response of SMB and melting in the following austral summer. The number of melt days derived from satellite data also gives 6-month lagged correlations to SOI that are as high or higher than

915 synchronous correlations for most ice shelves (dashed curves in Fig. 13b-h).

We now discuss possible explanations for this lag. As mentioned previously, the Rossby wave trains connecting the Equatorial Pacific to Antarctica are expected to develop within a few weeks in response to ENSO convective anomalies (e.g. Hoskins and Karoly, 1981; Mo and Higgins, 1998; Peters and Vargin, 2015). Therefore, the lag has to come from anomalies stored in a slower medium, such as

920 snowpack, ocean, or sea ice. Snow surface melting in DJF is neither correlated to the temperature of snow layers within the first 2m in the previous months (not shown), nor to the snow accumulated over the previous months (not shown). This indicates that heat diffusion in snow or preconditioned porosity or albedo of snow are not responsible for the 6-month lag. By contrast, we find that El Niño events in JJA significantly reduce the sea ice cover in the following DJF (Fig. 14). This is reminiscent of Clem et al.,

925 (2017) who found stronger lagged correlation between SON ENSO and DJF sea ice cover than synchronous correlation in DJF, with consequences on summer air temperatures. We suggest two possible explanations for this lagged ENSO-sea-ice relationship. First, it could be slowly advected from the Ross Sea. Pope et al., (2017) indeed found that El Niño events developing in MAM created a dipole of sea ice anomalies, with decreased (increased) concentration in the Ross Sea (Amundsen and Bellingshausen

930 Seas). Using a novel sea ice budget analysis, they showed that the decreased concentration in the Ross Sea was then advected eastward, reaching the Amundsen Sea in SON and DJF. There is also another possible pathway for lagged ENSO/sea-ice relationship. The zonal wind stress over the Amundsen Sea continental shelf break is a good proxy for the transport of Circumpolar Deep Water (CDW) onto the continental shelf (Thoma et al., 2008; Holland et al., 2019). Steig et al., (2012) noted significant

935 correlations between that wind stress and ENSO in JJA and SON but not in DJF. All these studies as well

Supprimé: NINO34

Supprimé: investigate

Supprimé: NINO34

Supprimé: NINO34

Supprimé: NINO34

Supprimé: NINO34

Supprimé: NINO34

Supprimé: media, i.e. snow, ocean, or sea ice. We do not find any significant correlation between snow surface melting in DJF and the temperature of snow layers within the first 2m in the previous months (not shown), which indicates that heat diffusion in snow is not responsible for the 6-month lag. A part of the ENSO signature in austral winter could alternatively been stored in the ocean sub-surface layers as a result of wind stress anomalies (Steig et al., 2012). While ocean water masses can reside 6 months over the Amundsen continental shelf, the ocean is usually strongly stratified in summer, i.e. surface waters are disconnected from the sub-surface, and it is not obvious that anomalies stored in the sub-surface can affect the surface air properties. A possible mechanism for this is the meltwater pump described by Jourdain et al. (2017) and St-Laurent et al. (2017) whereby increased melting at the base of ice shelves favors the entrainment of warm deep waters towards the surface. Increased marine intrusion of CDW associated with El Niño events (Paolo et al., 2018; Steig et al., 2012) may take approximately 6 months to reach the ice-shelf base, where they would increase basal melting, thereby entraining warm water towards the surface, decreasing the sea ice volume near the ice-shelf fronts (as described by Jourdain et al. 2017 and Merino et al. 2018), warming surface waters, hence favoring moisture supply to the atmosphere via increased evaporation. Pope et al. (2017) found a reduced DJF sea ice cover during El Niño events, which would support this mechanism, but they provided another explanation. They showed that the sea ice cover was affected by ENSO in the Ross Sea in austral winter, with an anomaly that was slowly advected eastward over the next 6 months. Their mechanism would also explain the 6 months lag independently from sub-surface ocean anomalies.

as Paolo et al., (2018) pointed out scales of a few months for the buildup and advection of CDW on the continental shelf then into the ice shelf cavities where they produce basal melting, and Paolo et al., (2018) reported correlations between ENSO and ice shelf thinning 6 months later. As stronger ice-shelf melt rates tend to decrease sea ice in this region due to the entrainment of warm CDW towards the surface (Jourdain et al., 2017; Merino et al., 2018), the connection through CDW intrusions may also explain a part of the lag between ENSO and DJF sea ice in the Amundsen Sea. We suggest that both mechanisms (eastward advection of sea ice anomalies and anomalous intrusions of CDW) may explain the 6-month lag between DJF SMB or melting and ENSO, and we leave the details of the ocean/sea-ice processes for future research.

Beyond the ASL and ENSO, we also find that the SAM is not significantly related to summer SMB and surface melt over individual drainage basins at interannual time scales, which agrees with Deb et al. (2018). This may appear contradictory to the results obtained by Medley and Thomas (2019), showing that the positive SAM trend from 1957 to 2000 largely explains the pattern of annual SMB trends over the Antarctic ice sheet. First of all, their residual SMB trend (i.e. not related to SAM) is particularly strong in the Amundsen Sea Embayment (their Fig. 1e), highlighting that only a part of the SMB trend in that region may be related to the SAM trend. The multi-decadal SAM trend is also related to ozone depletion and emissions of greenhouse gases, and the interannual SAM variability may have different characteristics and impacts on SMB. Furthermore, the absence of SMB-SAM relationship in our MAR simulations is specific to the austral summer, (that represent 15% of the annual SMB), and correlations are more significant for the other seasons (Tab.S3 in supplementary material). Therefore, the significant SAM-SMB relationship suggested by Medley and Thomas (2009) for annual SMB are not necessarily in contradictory to our results. Lastly, previous studies have suggested that the SAM-ENSO anti-correlation may diminish the impact of ENSO on surface melting and SMB. Partial correlations used to disentangle the SAM and ENSO influences on SMB do indicate a slightly stronger SMB-ENSO correlation when the effect of SAM is removed (in particular for Abbot and Cosgrove, see 2<sup>nd</sup> and 3<sup>rd</sup> columns of Table 5), but the effect is relatively small. For melt rates, the SAM modulation is very weak for all the basins (Table 5, 4<sup>th</sup> and 5<sup>th</sup> columns).

Supprimé: ,

Supprimé: not shown

Supprimé: contradiction

Supprimé: Last

Supprimé: NINO34

Déplacé vers le bas [5]: [Table 5 : Partial Correlation of](#)

Déplacé vers le bas [6]: vs SMB or melt rates, removing the influence of SAM (columns 2 and 4). Corresponding full correlations are indicated in columns 3 and 5 (same as Table 3 and Table 4).[Table 4](#).

Supprimé: NINO34

Supprimé: Drainage Basins ... [9]

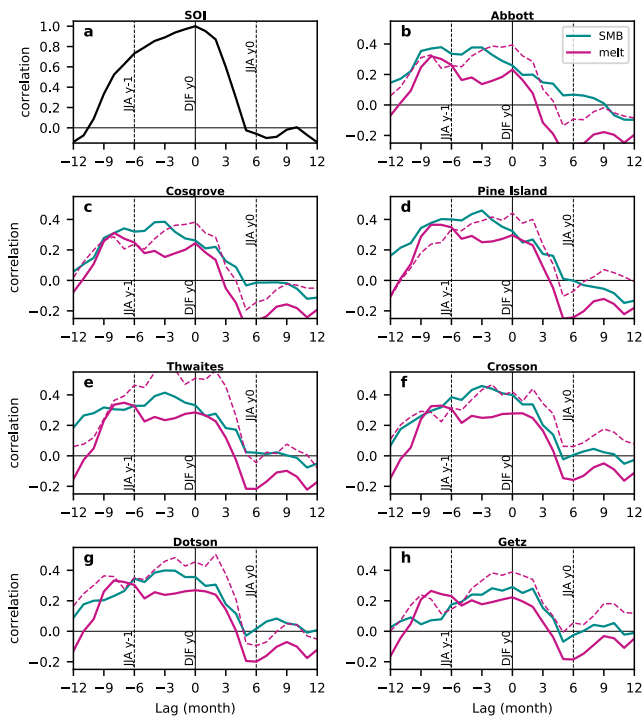


Figure 13 : Correlation between lagged 3-month averaged  $\text{SOI}$  (i.e. DJF at zero lag, previous JJA at -6 lag) and (a) DJF  $\text{SOI}$ , (b-h) simulated SMB and melt rates in individual drainage basins. The dashed curves correspond to the number of melt days derived from satellite data by Picard et al. (2007).

Supprimé: 13

Supprimé: NINO34

Supprimé: NINO34

Déplacé (insertion) [5]

Déplacé (insertion) [6]

Table 5 : Partial Correlation of -SOI vs SMB or melt rates, removing the influence of SAM (columns 2 and 4). Corresponding full correlations are indicated in columns 3 and 5 (same as Table 3 and Table 4).

Drainage Basins	Partial correlation -SOI vs SMB (without SAM)	-SOI vs SMB	-SOI vs SMB	Partial correlation -SOI vs surface melt (without SAM)	Correlation -SOI vs surface melt
Abbot	0.36	0.25	0.21	0.23	0.23
Cosgrove	0.37	0.26	0.21	0.23	0.24
Pine Island	0.38	0.32	0.26	0.30	0.30
Thwaites	0.38	0.33	0.23	0.25	0.29
Crosson	0.45	0.40	0.29	0.24	0.28
Dotson	0.40	0.36	0.25	0.23	0.27
Getz	0.26	0.30	0.18	0.17	0.22

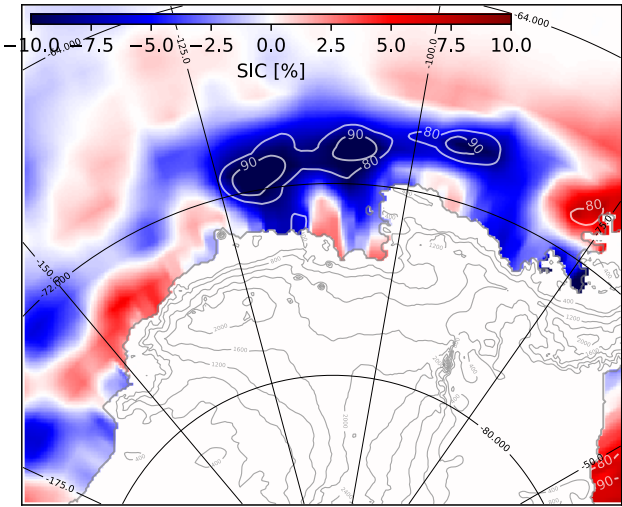


Figure 14 : Summer sea ice cover (%) anomaly (composites minus the climatology over 1979-2017) during El Niño events in JJA (6 month before). Contours represent significance with a t-test.

We now discuss the relationship between surface melt and SMB. According to Table 2, runoff is null over all drainage basins which mean that the firn is never saturated. All surface melt and rainfall refreeze within the annual snow layer. Surface melt needed to deplete all the air in the annual snow layer and lead to hydrofracturing can be defined as  $snowfall * [\rho_{water} / \rho_{snow}] * [1 - (\rho_{snow} / \rho_{ice})]$ , with snowfall in water equivalent, a fresh snow density of  $300 \text{ kg m}^{-3}$  and ice density of  $920 \text{ kg m}^{-3}$ . This indicates that meltwater ponding and complex surface hydrological flows are unlikely to develop over West Antarctic drainage basins with such amount of precipitation and surface water needed (between 991 and 2205  $\text{mm.w.e yr}^{-1}$  depending on the drainage basin). This would prevent surface hydrological flows, melt water ponding and ice-shelf collapse from hydrofracturing.

## 5 Conclusion

In this paper we have analyzed possible drivers for summer surface melt and SMB interannual variability over the last decades in the Amundsen sector, West Antarctica. For this, we have simulated the 1979 to 2017 period with the regional atmospheric model, MAR. We have first evaluated our model configuration in comparison to observational products (i.e. AWS, airborne-radar and firn-core SMB, melt days from satellite microwave, and melt rates from satellite scatterometer). MAR gives good results for near-surface temperatures (mean overestimation of  $0.10^\circ\text{C}$ ), near-surface wind speeds (mean underestimation of  $0.42 \text{ m s}^{-1}$ ), and SMB (local relative bias  $< 20\%$  over the Thwaites basin). The mean surface melt rate over the Amundsen Sea region is underestimated by 18% compared to the estimates derived from QuickSCAT (Trusel et al., 2013), and the interannual variability of surface melting is relatively well reproduced in terms of melt rate ( $R=0.80$ ) or number of melt days ( $R=0.43$  to  $0.69$  depending on the satellite product) as also found by previous study using the same MAR version (i.e. Datta et al., 2019). Similar underestimation was also found in another regional atmospheric model of the Amundsen region (underestimation of 30–50% found by Lenaerts et al., 2017). Overall, our results indicate that MAR is a suitable tool to study interannual variability in the Amundsen sector.

Then, we have analyzed the interannual variability of summer SMB. The strongest summer SMB occurs over Thwaites and Pine Island glaciers when the ASL migrates far westward (by typically  $30^\circ$ ) and southward (by typically  $3-4^\circ$ ). This promotes a southward flow on the Eastern flank of the ASL, towards the glaciers, with resulting increased moisture convergence, precipitation, and therefore SMB. Our study hence provides further support for the connection between Antarctic precipitation and the ASL longitudinal position that was previously described by Hosking et al. (2013) based on the ERA-interim reanalysis. In terms of climate indices, this corresponds to an anti-correlation between SMB and the ASL longitudinal position. This anti-correlation is found for all the drainage basins of the Amundsen Sea Embayment, and the part of the SMB variance explained by the ASL longitudinal migrations ranges from 2 % to 41 % (increasing westward). A small part of the SMB variance is also related to ENSO, with higher

Supprimé: over

Supprimé: in

Supprimé: Strongest

SMB during El Niño events and lower SMB during La Niña, but less than 8% of the SMB variance is explained by ENSO variability. This SMB connection to ENSO is independent from its connection the ASL longitudinal position.

1070 We have also analyzed the interannual variability of summer surface melt rates. Strongest surface melting occurs over Thwaites and Pine Island glaciers when the ASL undergoes an anticyclonic anomaly (likely the signature of blocking activity), which is visible through anomalies of the ASL relative central pressure. Such an anomaly promotes a southward anomaly of near-surface winds anomaly and moisture convergence over the Amundsen Sea Embayment. As recently described by Scott et al. (2019), this leads

1075 to increased cloud cover and downward longwave radiation, which in turns increases surface melting. As for SMB, we do not find that surface melt rate variability in our simulations is strongly connected to ENSO as it does not explain more than 9% of the total variance in simulated summer surface melt rate (or 12% of the number of melt days). By contrast, and for unknown reasons, the variance in number of melt days derived from satellite products indicates that as much as 25% of the variance in these products

1080 could be explained by SOI.

We also suggest that at least a part of the ENSO-SMB and ENSO-melt relationships in summer is inherited from the previous austral winter (JJA). Rossby wave trains generated by convective anomalies related to developing El Niño events in austral winter significantly affect the Antarctic region and we suggest that this has some impact on SMB and surface melting in the Amundsen sector 6 months later.

1085 Such delay could either be related to sea ice anomalies generated by ENSO in the Ross Sea in austral winter and taking 6 months to be advected to the Amundsen Sea (Pope et al., 2017), or to marine intrusions of Circumpolar Deep Water that are favored by El Niño events in austral winter (Steig et al., 2012). Circumpolar Deep Water may take 6 months to reach ice shelf cavities where increased basal melting favors the entrainment of this water towards the ocean surface (Jourdain et al., 2017).

1090 We lastly propose that the rate of surface water production (rainfall + melting) would need to increase by nearly two orders of magnitude to saturate present-day annual snow layer and therefore to initiate hydrofracturing. This is possible for strong warming scenarios given the exponential temperature dependence described by Trusel et al., (2015) , although snowfall is also expected to increase (Krinner et al., 2008; Agosta et al., 2013; Ligtenberg et al., 2013; Lenaerts et al., 2016; Palerme et al., 2017), requiring

1095 even more meltwater to reach saturation.

- Supprimé: 8
- Supprimé: .
- Supprimé: ,
- Supprimé: NINO34
- Supprimé: and
- Supprimé:
- Supprimé: warm deep
- Supprimé: Saut de page



**Code and data availability:** The MAR code (version 3.9.1) is available on the MAR website (<http://mar.cnrs.fr/>), outputs from the Amundsen simulation presented in this study are available on <https://doi.org/10.5281/zenodo.2815907>.

**Author contributions:** The study was designed by Marion Donat-Magnin and Nicolas C. Jourdain. Set-up of the MAR domain configuration was made by Marion Donat-Magnin, Cécile Agosta, Amine Drira and Nicolas C. Jourdain. Cécile Agosta, Xavier Fettweis, Hubert Gallée, Christoph Kittel and Charles Amory developed and tuned the MAR model for Antarctica, and they contributed to improving and interpreting our simulations. Christoph Kittel developed the scripts used to compare MAR to AWS data. Jonathan D. Wille and Vincent Favier contributed to the interpretation of our results related to interannual variability. All the authors significantly contributed to this manuscript.

**Competing interests:** The authors declare that they have no conflict of interests.

**Acknowledgements:** This work was funded by the French National Research Agency (ANR) through the TROIS-AS (ANR-15-CE01-0005-01) project. The development of MAR was partly funded by Labex OSUG@2020 (ANR10 LABX56) through the “Tout le Monde se MAR” project. All the computations presented in this paper were performed using the GRICAD infrastructure (<https://gricad.univ-grenoble-alpes.fr>), which is partly supported by the Equip@Meso project (ANR-10-EQPX-29-01) of the program “Investissements d’Avenir” supervised by ANR, by the Rhône-Alpes region (GRANT CPER07\_13 CIRA: <http://www.ci-ra.org>) and by France-Grilles (<http://www.france-grilles.fr>). We thank G. Picard, L. Trusel, J. Nicolas, Y. Wang and B. Medley for making their data available.

Supprimé: ¶

## References

- 1135 [Agosta, C., Favier, V., Krinner, G., Gallée, H., Fettweis, X. and Genthon, C.: High-resolution modelling of the Antarctic surface mass balance, application for the twentieth, twenty first and twenty second centuries, \*Climate dynamics\*, 41\(11–12\), 3247–3260, doi:10.1007/s00382-013-1903-9, 2013.](#)
- 1140 Agosta, C., Amory, C., Kittel, C., Orsi, A., Favier, V., Gallée, H., Broeke, M., Lenaerts, J., Wessem, J. and Fettweis, X.: Estimation of the Antarctic surface mass balance using MAR (1979–2015) and identification of dominant processes, *The Cryosphere Discussions*, 1–22, doi:https://doi.org/10.5194/tc-13-281-2019, 2019.
- 1145 Amory, C., Trouvilliez, A., Gallée, H., Favier, V., Naaim-Bouvet, F., Genthon, C., Agosta, C., Piard, L. and Bellot, H.: Comparison between observed and simulated aeolian snow mass fluxes in Adélie Land, East Antarctica, *The Cryosphere Discussions*, (9), 1373–1383, doi:https://doi.org/10.5194/tc-9-1373-2015, 2015.
- 1150 Asay-Davis, X. S., Jourdain, N. C. and Nakayama, Y.: Developments in simulating and parameterizing interactions between the Southern Ocean and the Antarctic Ice sheet, *Current Climate Change Reports*, 3(4), 316–329, doi:https://doi.org/10.1007/s40641-017-0071-0, 2017.
- Bell, R. E., Banwell, A. F., Trusel, L. D. and Kingslake, J.: Antarctic surface hydrology and impacts on ice-sheet mass balance, *Nature Climate Change*, 1, doi:https://doi.org/10.1038/s41558-018-0326-3, 2018.
- 1155 Bracegirdle, T. J., Connolley, W. M. and Turner, J.: Antarctic climate change over the twenty first century, *Journal of Geophysical Research (Atmospheres)*, 113, doi:https://doi.org/10.1029/2007jd008933, 2008.
- 1160 Van den Broeke, M.: Strong surface melting preceded collapse of Antarctic Peninsula ice shelf: Melting on Antarctic ice shelves, *Geophysical Research Letters*, 32(12), doi:10.1029/2005GL023247, 2005.
- 1165 Bromwich, D. H., Rogers, A. N., Källberg, P., Cullather, R. I., White, J. W. and Kreutz, K. J.: ECMWF analyses and reanalyses depiction of ENSO signal in Antarctic precipitation, *Journal of Climate*, 13(8), 1406–1420, doi:https://doi.org/10.1175/15200442(2000)013<1406:EAARDO>2.0.CO;2, 2000.
- Bromwich, D. H., Nicolas, J. P. and Monaghan, A. J.: An Assessment of Precipitation Changes over Antarctica and the Southern Ocean since 1989 in Contemporary Global Reanalyses, *Journal of Climate*, 24, 4189–4209, 2011.
- 1170 Bromwich, D. H., Nicolas, J. P., Monaghan, A. J., Lazzara, M. A., Keller, L. M., Weidner, G. A. and Wilson, A. B.: Central West Antarctica among the most rapidly warming regions on Earth, *Nature Geoscience*, 6(2), 139–145, doi:10.1038/ngeo1671, 2013.
- 1175 Brun, E., David, P., Sudul, M. and Brunot, G.: A numerical model to simulate snow-cover stratigraphy for operational avalanche forecasting, *Journal of Glaciology*, 38(128), 13–22, doi:https://doi.org/10.1017/s0022143000009552, 1992.
- 1180 Cai, W., Borlace, S., Lengaigne, M., Van Rensch, P., Collins, M., Vecchi, G., Timmermann, A., Santoso, A., McPhaden, M. J., Wu, L. and others: Increasing frequency of extreme El Niño events due to greenhouse warming, *Nature climate change*, 4(2), 111, doi:https://doi.org/10.1038/nclimate2100, 2014.

- 1185 Cai, W., Wang, G., Santoso, A., Lin, X. and Wu, L.: Definition of extreme El Niño and its impact on  
projected increase in extreme El Niño frequency, *Geophysical Research Letters*, 44(21),  
doi:<https://doi.org/10.1002/2017gl075635>, 2017.
- 1190 Clem, K. R., Renwick, J. A. and McGregor, J.: Large-Scale Forcing of the Amundsen Sea Low and Its  
Influence on Sea Ice and West Antarctic Temperature, *J. Climate*, 30(20), 8405–8424,  
doi:[10.1175/JCLI-D-16-0891.1](https://doi.org/10.1175/JCLI-D-16-0891.1), 2017.
- Chen, G. and Held, I. M.: Phase speed spectra and the recent poleward shift of Southern Hemisphere  
surface westerlies, *Geophysical Research Letters*, 34(21), doi:<https://doi.org/10.1029/2007gl031200> ,  
2007.
- 1195 Cullather, R. I., Bromwich, D. H. and Van Woert, M. L.: Interannual variations in Antarctic  
precipitation related to El Niño-Southern Oscillation, *Journal of Geophysical Research: Atmospheres*,  
101(D14), 19109–19118, doi:<https://doi.org/10.1029/96jd01769>, 1996.
- 1200 Datta, R. T., Tedesco, M., Fettweis, X., Agosta, C., Lhermitte, S., Lenaerts, J. and Wever, N.: The  
Effect of Foehn-Induced Surface Melt on Firn Evolution Over the Northeast Antarctic Peninsula,  
*Geophysical Research Letters*, 46, doi:[10.1029/2018GL080845](https://doi.org/10.1029/2018GL080845), 2019.
- 1205 De Ridder, K. and Gallée, H.: Land surface–induced regional climate change in southern Israel, *Journal  
of applied meteorology*, 37(11), 1470–1485,  
doi:[https://doi.org/10.1175/15200450\(1998\)037<1470:lsircc>2.0.co;2](https://doi.org/10.1175/15200450(1998)037<1470:lsircc>2.0.co;2), 1998.
- Deb, P., Orr, A., Bromwich, D. H., Nicolas, J. P., Turner, J. and Hosking, J. S.: Summer drivers of  
atmospheric variability affecting ice shelf thinning in the Amundsen Sea Embayment, West Antarctica,  
1210 *Geophysical Research Letters*, 45(9), 4124–4133, doi: <https://doi.org/10.1029/2018gl077092>, 2018.
- Deconto, R. M. and Pollard, D.: Contribution of Antarctica to past and future sea-level rise, *Nature*,  
531, 591–597, doi:[10.1038/nature17145](https://doi.org/10.1038/nature17145), doi:[10.1038/nature17145](https://doi.org/10.1038/nature17145), 2016.
- 1215 Dee, D. P., Uppala, S., Simmons, A., Berrisford, P., Poli, P., Kobayashi, S., Andrae, U., Balmaseda, M.,  
Balsamo, G., Bauer, d P. and others: The ERA-Interim reanalysis: Configuration and performance of  
the data assimilation system, *Quarterly Journal of the royal meteorological society*, 137(656), 553–597,  
doi:<https://doi.org/10.1002/qj.493>, 2011.
- 1220 Deser, C., Phillips, A. S., Tomas, R. A., Okumura, Y. M., Alexander, M. A., Capotondi, A., Scott, J. D.,  
Kwon, Y.-O. and Ohba, M.: ENSO and Pacific Decadal Variability in the Community Climate System  
Model Version 4, *Journal of Climate*, 25, 2622–2651, doi:<https://doi.org/10.1175/jcli-d-11-00301.1>,  
2012.
- 1225 Ding, Q., Steig, E. J., Battisti, D. S. and Küttel, M.: Winter warming in West Antarctica caused by  
central tropical Pacific warming, *Nature Geoscience*, 4(6), 398, doi:<https://doi.org/10.1038/ngeo1129>,  
2011.
- 1230 Dutrieux, P., De Rydt, J., Jenkins, A., Holland, P. R., Ha, H. K., Lee, S. H., Steig, E. J., Ding, Q.,  
Abrahamsen, E. P. and Schröder, M.: Strong sensitivity of Pine Island ice-shelf melting to climatic  
variability, *Science*, 343(6167), 174–178, doi: <https://doi.org/10.1126/science.1244341>, 2014.
- Edwards, T. L., Brandon, M. A., Durand, G., Edwards, N. R., Golledge, N. R., Holden, P. B., Nias, I. J.,  
Payne, A. J., Ritz, C. and Wernecke, A.: Revisiting Antarctic ice loss due to marine ice-cliff instability,  
1235 *Nature*, 566(7742), 58, doi:<https://doi.org/10.1038/s41586-019-0901-4>, 2019.
- Favier, L., Durand, G., Cornford, S., Gudmundsson, G., Gagliardini, O., Gillet-Chaulet, F., Zwinger, T.,

- Payne, A. and Le Brocq, A.: Retreat of Pine Island Glacier controlled by marine ice-sheet instability, *Nature Climate Change*, 4(2), 117–121, doi: <https://doi.org/10.1038/nclimate2094>, 2014.
- 1240 Favier, V., Agosta, C., Parouty, S., Durand, G., Delaygue, G., Gallee, H., Drouet, A. S., Trouvilliez, A. and Krinner, G.: An updated and quality controlled surface mass balance dataset for Antarctica, *The Cryosphere*, 7(2), 583–597, doi:10.5194/tc-7-583-2013, 2013.
- 1245 Favier, V., Krinner, G., Amory, C., Gallée, H., Beaumet, J. and Agosta, C.: Antarctica-Regional Climate and Surface Mass Budget, *Current Climate Change Reports*, 3(4), 303–315, <https://doi.org/10.1007/s40641-017-0072-z>, 2017.
- 1250 Fettweis, X., Box, J., Agosta, C., Amory, C., Kittel, C., Lang, C., van As, D., Machguth, H. and Gallée, H.: Reconstructions of the 1900–2015 Greenland ice sheet surface mass balance using the regional climate MAR model, *Cryosphere (The)*, 11, 1015–1033, doi:<https://doi.org/10.5194/tc-2016-268>, 2017.
- Fogt, R. L. and Wovrosh, A. J.: The Relative Influence of Tropical Sea Surface Temperatures and Radiative Forcing on the Amundsen Sea Low, *Journal of Climate*, 28(21), 8540–8555, doi: <https://doi.org/10.1175/jcli-d-15-0091.1>, 2015.
- 1255 Fogt, R. L., Bromwich, D. H. and Hines, K. M.: Understanding the SAM influence on the South Pacific ENSO teleconnection, *Climate Dynamics*, 36, 1555–1576, doi: <https://doi.org/10.1007/s00382-010-0905-0>, 2011.
- 1260 Fretwell, P., Pritchard, H. D., Vaughan, D. G., Bamber, J. L., Barrand, N. E., Bell, R., Bianchi, C., Bingham, R. G., Blankenship, D. D., Casassa, G., Catania, G., Callens, D., Conway, H., Cook, A. J., Corr, H. F. J., Damaske, D., Damm, V., Ferraccioli, F., Forsberg, R., Fujita, S., Gim, Y., Gogineni, P., Griggs, J. A., Hindmarsh, R. C. A., Holmlund, P., Holt, J. W., Jacobel, R. W., Jenkins, A., Jokat, W., Jordan, T., King, E. C., Kohler, J., Krabill, W., Riger-Kusk, M., Langley, K. A., Leitchenkov, G., 1265 Leuschen, C., Luyendyk, B. P., Matsuoka, K., Mouginot, J., Nitsche, F. O., Nogi, Y., Nost, O. A., Popov, S. V., Rignot, E., Rippin, D. M., Rivera, A., Roberts, J., Ross, N., Siegert, M. J., Smith, A. M., Steinhage, D., Studinger, M., Sun, B., Tinto, B. K., Welch, B. C., Wilson, D., Young, D. A., Xiangbin, C. and Zirizzotti, A.: Bedmap2: improved ice bed, surface and thickness datasets for Antarctica, *The Cryosphere*, 7(1), 375–393, doi:10.5194/tc-7-375-2013, 2013.
- 1270 Fyke, J., Lenaerts, J. and Wang, H.: Basin-scale heterogeneity in Antarctic precipitation and its impact on surface mass variability, *The Cryosphere*, 11(6), 2595–2609, doi:<https://doi.org/10.5194/tc-11-2595-2017>, 2017.
- 1275 Gallée, H.: Simulation of the mesocyclonic activity in the Ross Sea, Antarctica, *Monthly Weather Review*, 123(7), 2051–2069, doi:[https://doi.org/10.1175/1520-0493\(1995\)123<2051:sotmai>2.0.co;2](https://doi.org/10.1175/1520-0493(1995)123<2051:sotmai>2.0.co;2), 1995.
- 1280 Gallée, H. and Gorodetskaya, I. V.: Validation of a limited area model over Dome C, Antarctic Plateau, during winter, *Climate dynamics*, 34(1), 61, doi:<https://doi.org/10.1007/s00382-008-0499-y>, 2010.
- Gallée, H. and Schayes, G.: Development of a three-dimensional meso- $\gamma$  primitive equation model: katabatic winds simulation in the area of Terra Nova Bay, Antarctica, *Monthly Weather Review*, 122(4), 671–685, doi:[https://doi.org/10.1175/1520-0493\(1994\)122<0671:doatdm>2.0.co;2](https://doi.org/10.1175/1520-0493(1994)122<0671:doatdm>2.0.co;2), 1994.
- 1285 Gallée, H., Preunkert, S., Argentini, S., Frey, M., Genthon, C., Jourdain, B., Pietroni, I., Casasanta, G., Barral, H., Vignon, E. and others: Characterization of the boundary layer at Dome C (East Antarctica) during the OPALE summer campaign, *Atmospheric Chemistry and Physics*, 15(11), 6225–6236, doi:<https://doi.org/10.5194/acpd-14-33089-2014>, 2015.
- 1290 Genthon, C. and Cosme, E.: Intermittent signature of ENSO in west-Antarctic precipitation,

- Geophysical Research Letters, 30, doi:<https://doi.org/10.1029/2003gl018280>, 2003.
- 1295 Harangozo, S. A.: The relationship of Pacific deep tropical convection to the winter and springtime extratropical atmospheric circulation of the South Pacific in El Niño events, *Geophysical Research Letters*, 31(5), doi:10.1029/2003GL018667, 2004.
- 1300 Hartmann, D. L. and Lo, F.: Wave-driven zonal flow vacillation in the Southern Hemisphere, *Journal of the Atmospheric Sciences*, 55(8), 1303–1315, doi: [https://doi.org/10.1175/1520-0469\(1998\)055<1303:wdzfv>2.0.co;2](https://doi.org/10.1175/1520-0469(1998)055<1303:wdzfv>2.0.co;2), 1998.
- 1305 Holland, P. R., Bracegirdle, T. J., Dutrieux, P., Jenkins, A. and Steig, E. J.: West Antarctic ice loss influenced by internal climate variability and anthropogenic forcing, *Nature Geoscience*, 12(9), 718–724, doi:10.1038/s41561-019-0420-9, 2019.
- 1310 Hosking, J. S., Orr, A., Marshall, G. J., Turner, J. and Phillips, T.: The influence of the Amundsen–Bellingshausen Seas low on the climate of West Antarctica and its representation in coupled climate model simulations, *Journal of Climate*, 26(17), 6633–6648, doi: <https://doi.org/10.1175/jcli-d-12-00813.1>, 2013.
- 1315 Hosking, J. S., Orr, A., Bracegirdle, T. J. and Turner, J.: Future circulation changes off West Antarctica: Sensitivity of the Amundsen Sea Low to projected anthropogenic forcing, *Geophysical Research Letters*, 43(1), 367–376, doi:<https://doi.org/10.1002/2015gl067143>, 2016.
- 1320 Hoskins, B. J. and Karoly, D. J.: The steady linear response of a spherical atmosphere to thermal and orographic forcing, *Journal of the Atmospheric Sciences*, 38(6), 1179–1196, doi:[https://doi.org/10.1175/1520-0469\(1981\)038<1179:tslroa>2.0.co;2](https://doi.org/10.1175/1520-0469(1981)038<1179:tslroa>2.0.co;2), 1981.
- 1325 Huai, B., Wang, Y., Ding, M., Zhang, J. and Dong, X.: An assessment of recent global atmospheric reanalyses for Antarctic near surface air temperature, *Atmospheric Research*, 226, 181–191, doi:10.1016/j.atmosres.2019.04.029, 2019.
- 1330 Izumo, T., Vialard, J., Lengaigne, M., de Boyer Montegut, C., Behera, S. K., Luo, J.-J., Cravatte, S., Masson, S. and Yamagata, T.: Influence of the state of the Indian Ocean Dipole on the following year’s El Niño, *Nature Geoscience*, 3(3), 168, doi:<http://dx.doi.org/10.1038/ngeo760>, 2010.
- 1335 Jacobs, S., Jenkins, A., Hellmer, H., Giulivi, C., Nitsche, F., Huber, B. and Guerrero, R.: The Amundsen Sea and the Antarctic ice sheet, *Oceanography*, 25(3), 154–163, doi: <https://doi.org/10.5670/oceanog.2012.90>, 2012.
- 1340 Jenkins, A., Dutrieux, P., Jacobs, S., Steig, E. J., Gudmundsson, G. H., Smith, J. and Heywood, K. J.: Decadal Ocean Forcing and Antarctic Ice Sheet Response: Lessons from the Amundsen Sea, *Oceanography*, 29(4), 106–117, 2016.
- 1345 Jenkins, A., Shoosmith, D., Dutrieux, P., Jacobs, S., Kim, T. W., Lee, S. H., Ha, H. K. and Stammerjohn, S.: West Antarctic Ice Sheet retreat in the Amundsen Sea driven by decadal oceanic variability, *Nature Geoscience*, 11, 733–738, doi: 10.1038/s41561-018-0207-4, 2018.
- 1350 Jones, J. M., Gille, S. T., Goosse, H., Abram, N. J., Canziani, P. O., Charman, D. J., Clem, K. R., Crosta, X., de Lavergne, C., Eisenman, I. and others: Assessing recent trends in high-latitude Southern Hemisphere surface climate, *Nature Climate Change*, 6(10), 917–926, doi:<https://doi.org/10.1038/nclimate3103>, 2016.
- 1355 Joughin, I., Smith, B. E. and Holland, D. M.: Sensitivity of 21st century sea level to ocean-induced thinning of Pine Island Glacier, Antarctica, *Geophysical Research Letters*, 37(20),doi:

- <https://doi.org/10.1029/2010gl044819>, 2010.
- Joughin, I., Smith, B. E. and Medley, B.: Marine ice sheet collapse potentially under way for the Thwaites Glacier Basin, West Antarctica, *Science*, 344(6185), 735–738, doi: 1350 810 <https://doi.org/10.1126/science.1249055>, 2014.
- Jourdain, N. C., Mathiot, P., Merino, N., Durand, G., Le Sommer, J., Spence, P., Dutrieux, P. and Madec, G.: Ocean circulation and sea-ice thinning induced by melting ice shelves in the Amundsen Sea, *Journal of Geophysical Research: Oceans*, doi: <https://doi.org/10.1002/2016jc012509>, 2017. 1355
- Kingslake, J., Ely, J. C., Das, I. and Bell, R. E.: Widespread movement of meltwater onto and across Antarctic ice shelves, *Nature*, 544(7650), 349, doi:<https://doi.org/10.1038/nature22049>, 2017.
- Kittel, C., Amory, C., Agosta, C., Delhasse, A., Doutreloup, S., Huot, P.-V., Wyard, C., Fichet, T. and Fettweis, X.: Sensitivity of the current Antarctic surface mass balance to sea surface conditions using MAR, *Cryosphere (The)*, 12, 3827–3839, doi:10.5194/tc-12-3827-2018, 2018. 1360
- Krinner, G., Guicherd, B., Ox, K., Genthon, C. and Magand, O.: Influence of Oceanic Boundary Conditions in Simulations of Antarctic Climate and Surface Mass Balance Change during the Coming Century, *Journal of Climate*, 21(5), 938–962, doi:10.1175/2007jcli1690.1, 2008. 1365
- Lang, C., Fettweis, X. and Erpicum, M.: Future projections of the climate and surface mass balance of Svalbard with the regional climate model MAR., *Cryosphere Discussions*, 9(1), doi:<https://doi.org/10.5194/tcd-9-115-2015>, 2015. 1370
- Lachlan-Cope, T. and Connolley, W.: Teleconnections between the tropical Pacific and the Amundsen-Bellinghausens Sea: Role of the El Niño/Southern Oscillation, *Journal of Geophysical Research (Atmospheres)*, 111(D10), 2006.
- Lenaerts, J., den Broeke, M., Déry, S., Meijgaard, E., Berg, W., Palm, S. P. and Sanz Rodrigo, J.: Modeling drifting snow in Antarctica with a regional climate model: 1. Methods and model evaluation, *Journal of Geophysical Research: Atmospheres*, 117(D5), doi:<https://doi.org/10.1029/2011jd016145>, 2012. 1375
- Lenaerts, J. T., Vizcaino, M., Fyke, J., Van Kampenhout, L. and van den Broeke, M. R.: Present-day and future Antarctic ice sheet climate and surface mass balance in the Community Earth System Model, *Climate Dynamics*, 47(5–6), 1367–1381, doi:10.1007/s00382-015-2907-4, 2016. 1380
- Lenaerts, J. T., Ligtenberg, S. R., Medley, B., Van de Berg, W. J., Konrad, H., Nicolas, J. P., Van Wessem, J. M., Trusel, L. D., Mulvaney, R., Tuckwell, R. J. and others: Climate and surface mass balance of coastal West Antarctica resolved by regional climate modelling, *Annals of Glaciology*, 1–13, doi:<https://doi.org/10.1017/aog.2017.42>, 2017. 1385
- Ligtenberg, S., Van de Berg, W., Van den Broeke, M., Rae, J. and Van Meijgaard, E.: Future surface mass balance of the Antarctic ice sheet and its influence on sea level change, simulated by a regional atmospheric climate model, *Climate dynamics*, 41(3–4), 867–884, <https://doi.org/10.1007/s00382-013-1749-1>, 2013. 1390
- Limpasuvan, V. and Hartmann, D. L.: Eddies and the annular modes of climate variability, *Geophysical Research Letters*, 26(20), 3133–3136, doi: <https://doi.org/10.1029/1999gl010478>, 1999. 1395
- Marshall, G. J.: Trends in the Southern Annular Mode from observations and reanalyses, *Journal of Climate*, 16(24), 4134–4143, doi: [https://doi.org/10.1175/1520-0442\(2003\)016<4134:titsam>2.0.co;2](https://doi.org/10.1175/1520-0442(2003)016<4134:titsam>2.0.co;2) 2003.

- 1400 Medley, B. and Thomas, E.: Increased snowfall over the Antarctic Ice Sheet mitigated twentieth-century sea-level rise, *Nature Climate Change*, 9(1), 34, doi:<https://doi.org/10.1038/s41558-018-0356-x>, 2019.
- 1405 Medley, B., Joughin, I., Das, S., Steig, E., Conway, H., Gogineni, S., Criscitiello, A., McConnell, J., Smith, B., Broeke, M. and others: Airborne-radar and ice-core observations of annual snow accumulation over Thwaites Glacier, West Antarctica confirm the spatiotemporal variability of global and regional atmospheric models, *Geophysical Research Letters*, 40, 3649–3654, doi: <https://doi.org/10.1002/grl.50706>, 2013.
- 1410 Medley, B., Joughin, I., Smith, B., Das, S. B., Steig, E. J., Conway, H., Gogineni, S., Lewis, C., Criscitiello, A. S., McConnell, J. R. and others: Constraining the recent mass balance of Pine Island and Thwaites glaciers, West Antarctica, with airborne observations of snow accumulation, *The Cryosphere*, 8(4), 1375–1392, doi:<https://doi.org/10.5194/tcd-8-953-2014>, 2014.
- 1415 Merino, N., Jourdain, N. C., Le Sommer, J., Goosse, H., Mathiot, P. and Durand, G.: Impact of increasing antarctic glacial freshwater release on regional sea-ice cover in the Southern Ocean, *Ocean Modelling*, 121, 76–89, doi:<https://doi.org/10.1016/j.ocemod.2017.11.009>, 2018.
- 1420 Mo, K. C. and Higgins, R. W.: The Pacific–South American Modes and Tropical Convection during the Southern Hemisphere Winter, *Monthly Weather Review*, 126(6), 1581–1596, doi:10.1175/1520-0493, 1998.
- 1425 Mougnot, J., Rignot, E. and Scheuchl, B.: Sustained increase in ice discharge from the Amundsen Sea Embayment, West Antarctica, from 1973 to 2013, *Geophysical Research Letters*, 41(5), 1576–1584, doi: <https://doi.org/10.1002/2013gl059069>, 2014.
- Newman, M., Shin, S.-I. and Alexander, M. A.: Natural variation in ENSO flavors, *Geophysical Research Letters*, 38(14), doi:<https://doi.org/10.1029/2011gl047658>, 2011.
- 1430 Nicolas, J. P. and Bromwich, D. H.: Climate of West Antarctica and Influence of Marine Air Intrusions, *J. Climate*, 24(1), 49–67, doi:10.1175/2010JCLI3522.1, 2010.
- 1435 Nicolas, J. P., Vogelmann, A. M., Scott, R. C., Wilson, A. B., Cadeddu, M. P., Bromwich, D. H., Verlinde, J., Lubin, D., Russell, L. M., Jenkinson, C. and others: January 2016 extensive summer melt in West Antarctica favoured by strong El Niño, *Nature communications*, 8, ncomms15799, doi: <https://doi.org/10.1038/ncomms15799>, 2017.
- 1440 Palerme, C., Genthon, C., Claud, C., Kay, J. E., Wood, N. B. and L’Ecuyer, T.: Evaluation of current and projected Antarctic precipitation in CMIP5 models, *Climate Dynamics*, 48, 225–239, doi:10.1007/s00382-016-3071-1, 2017.
- 1445 Paolo, F., Padman, L., Fricker, H., Adusumilli, S., Howard, S. and Siegfried, M.: Response of Pacific-sector Antarctic ice shelves to the El Niño/Southern Oscillation, *Nature Geoscience*, 11, 121–126, doi: <https://doi.org/10.1038/s41561-017-0033-0>, 2018.
- Pattyn, F., Ritz, C., Hanna, E., Asay-Davis, X., DeConto, R., Durand, G., Favier, L., Fettweis, X., Goelzer, H., Gollledge, N. R. and others: The Greenland and Antarctic ice sheets under 1.5° C global warming, *Nature Climate Change*, 1, doi:<https://doi.org/10.1038/s41558-018-0305-8>, 2018.
- 1450 Peters, D. H. and Vargin, P.: Influence of subtropical Rossby wave trains on planetary wave activity over Antarctica in September 2002, *Tellus A: Dynamic Meteorology and Oceanography*, 67(1), 25875, doi:<https://doi.org/10.3402/tellusa.v67.25875>, 2015.



- Philander, S., Lau, N., Pacanowski, R. and Nath, M.: Two Different Simulations of the Southern Oscillation and El Niño with Coupled Ocean–Atmosphere General Circulation Models, *Philosophical Transactions of the Royal Society of London Series A*, 329, 167–177, doi:<https://doi.org/10.1098/rsta.1989.0068>, 1989.
- Picard, G. and Fily, M.: Surface melting observations in Antarctica by microwave radiometers: Correcting 26-year time series from changes in acquisition hours, *Remote sensing of environment*, 104(3), 325–336, doi:<https://doi.org/10.1016/j.rse.2006.05.010>, 2006.
- Picard, G., Fily, M. and Gallée, H.: Surface melting derived from microwave radiometers: a climatic indicator in Antarctica, *Annals of Glaciology*, 46, 29–34, doi:<https://doi.org/10.3189/172756407782871684>, 2007.
- Pope, J. O., Holland, P. R., Orr, A., Marshall, G. J. and Phillips, T.: The impacts of El Niño on the observed sea ice budget of West Antarctica, *Geophysical Research Letters*, doi: <https://doi.org/10.1002/2017gl073414>, 2017.
- Pritchard, H., Ligtenberg, S., Fricker, H., Vaughan, D., Van den Broeke, M. and Padman, L.: Antarctic ice-sheet loss driven by basal melting of ice shelves, *Nature*, 484(7395), 502–505, doi: <https://doi.org/10.1038/nature10968>, 2012.
- Raphael, M., Marshall, G., Turner, J., Fogt, R., Schneider, D., Dixon, D., Hosking, J., Jones, J. and Hobbs, W.: The Amundsen Sea low: Variability, change, and impact on Antarctic climate, *Bulletin of the American Meteorological Society*, 97(1), 111–121, doi: <https://doi.org/10.1175/bams-d-14-00018.1>, 2016.
- Raphael, M. N. and Hobbs, W.: The influence of the large-scale atmospheric circulation on Antarctic sea ice during ice advance and retreat seasons, *Geophysical Research Letters*, 41(14), 5037–5045, doi:<https://doi.org/10.1002/2014gl060365>, 2014.
- Rignot, E., Mouginot, J., Scheuchl, B., van den Broeke, M., van Wessem, M. J. and Morlighem, M.: Four decades of Antarctic Ice Sheet mass balance from 1979–2017, *Proceedings of the National Academy of Sciences*, 116(4), 1095–1103, <https://doi.org/10.1073/pnas.1812883116>, 2019.
- Ritz, C., Edwards, T. L., Durand, G., Payne, A. J., Peyaud, V. and Hindmarsh, R. C.: Potential sea-level rise from Antarctic ice-sheet instability constrained by observations, *Nature*, 528(7580), 115–118, doi: <https://doi.org/10.1038/nature16147>, 2015.
- Ropelewski, C. F. and Jones, P. D.: An Extension of the Tahiti–Darwin Southern Oscillation Index, *Monthly Weather Review*, 115(9), 2161–2165, doi:10.1175/1520-0493(1987)115<2161:AEOTTS>2.0.CO;2, 1987.
- Roundy, P. E.: On the Interpretation of EOF Analysis of ENSO, Atmospheric Kelvin Waves, and the MJO, *J. Climate*, 28(3), 1148–1165, doi:10.1175/JCLI-D-14-00398.1, 2014.
- Scambos, T., Fricker, H. A., Liu, C.-C., Bohlander, J., Fastook, J., Sargent, A., Massom, R. and Wu, A.-M.: Ice shelf disintegration by plate bending and hydro-fracture: Satellite observations and model results of the 2008 Wilkins ice shelf break-ups, *Earth and Planetary Science Letters*, 280, 51–60, doi:10.1016/j.epsl.2008.12.027, 2009.
- Schoof, C.: Ice sheet grounding line dynamics: Steady states, stability, and hysteresis, *Journal of Geophysical Research: Earth Surface*, 112(F3), doi: <https://doi.org/10.1029/2006jf000664>, 2007.
- Scott, R. C., Nicolas, J. P., Bromwich, D. H., Norris, J. R. and Lubin, D.: Meteorological Drivers and

- Large-Scale Climate Forcing of West Antarctic Surface Melt, *Journal of Climate*, 32(3), 665–684, doi:<https://doi.org/10.1175/jcli-d-18-0233.1>, 2019.
- 1510 Scott Yiu, Y. Y. and Maycock, A. C.: On the Seasonality of the El Niño Teleconnection to the Amundsen Sea Region, *J. Climate*, 32(15), 4829–4845, doi:10.1175/JCLI-D-18-0813.1, 2019.
- 1515 Seroussi, H., Nakayama, Y., Larour, E., Menemenlis, D., Morlighem, M., Rignot, E. and Khazendar, A.: Continued retreat of Thwaites Glacier, West Antarctica, controlled by bed topography and ocean circulation, *Geophysical Research Letters*, n/a–n/a, doi:10.1002/2017GL072910, 2017.
- Shepherd, A. and Nowicki, S.: Improvements in ice-sheet sea-level projections, *Nature Climate Change*, 7, 672–674, 2017.
- 1520 Shepherd, A., Ivins, E., Rignot, E., Smith, B., van den Broeke, M., Velicogna, I., Whitehouse, P., Briggs, K., Joughin, I., Krinner, G. and others: Mass balance of the Antarctic ice sheet from 1992 to 2017., *Nature*., doi: <https://doi.org/10.1038/nclimate3400>, 2018.
- 1525 Steig, E. J., Schneider, D. P., Rutherford, S. D., Mann, M. E., Comiso, J. C. and Shindell, D. T.: Warming of the Antarctic ice-sheet surface since the 1957 International Geophysical Year, *Nature*, 457(7228), 459–462, doi:10.1038/nature07669, 2009.
- 1530 Steig, E. J., Ding, Q., Battisti, D. and Jenkins, A.: Tropical forcing of Circumpolar Deep Water inflow and outlet glacier thinning in the Amundsen Sea Embayment, West Antarctica, *Annals of Glaciology*, 53(60), 19–28, doi: <https://doi.org/10.3189/2012aog60a110>, 2012.
- 1535 St-Laurent, P., Yager, P., Sherrell, R., Stammerjohn, S. and Dinniman, M.: Pathways and supply of dissolved iron in the Amundsen Sea (Antarctica), *Journal of Geophysical Research: Oceans*, 122(9), 7135–7162, doi:<https://doi.org/10.1002/2017JC013162>, 2017.
- Tedesco, M.: Assessment and development of snowmelt retrieval algorithms over Antarctica from K-band spaceborne brightness temperature (1979–2008), *Remote Sensing of Environment*, 113(5), 979–997, doi:10.1016/j.rse.2009.01.009, 2009.
- 1540 Thoma, M., Jenkins, A., Holland, D. and Jacobs, S.: Modelling circumpolar deep water intrusions on the Amundsen Sea continental shelf, Antarctica, *Geophysical Research Letters*, 35(18), doi: <https://doi.org/10.1029/2008gl034939>, 2008.
- 1545 Thomas, E. R., Hosking, J. S., Tuckwell, R. R., Warren, R. A. and Ludlow, E. C.: Twentieth century increase in snowfall in coastal West Antarctica, *Geophysical Research Letters*, 42(21), 9387–9393, doi:10.1002/2015GL065750, 2015.
- 1550 Thompson, D. W. and Wallace, J. M.: Annular modes in the extratropical circulation. Part I: month-to-month variability\*, *Journal of Climate*, 13(5), 1000–1016, doi: [https://doi.org/10.1175/1520-0442\(2000\)013<1000:amitec>2.0.co;2](https://doi.org/10.1175/1520-0442(2000)013<1000:amitec>2.0.co;2), 2000.
- 1555 Torinesi, O., Fily, M. and Genthon, C.: Variability and trends of the summer melt period of Antarctic ice margins since 1980 from microwave sensors, *Journal of Climate*, 16(7), 1047–1060, doi:[https://doi.org/10.1175/1520-0442\(2003\)016<1047:vatots>2.0.co;2](https://doi.org/10.1175/1520-0442(2003)016<1047:vatots>2.0.co;2), 2003.
- Trusel, L. D., Frey, K. E. and Das, S. B.: Antarctic surface melting dynamics: Enhanced perspectives from radar scatterometer data, *Journal of Geophysical Research: Earth Surface*, 117(F2), doi:10.1029/2011JF002126, 2012.
- 1560 Trusel, L. D., Frey, K. E., Das, S. B., Munneke, P. K. and Broeke, M. R.: Satellite-based estimates of

- Antarctic surface meltwater fluxes, *Geophysical Research Letters*, 40(23), 6148–6153, doi:<https://doi.org/10.1002/2013gl058138>, 2013.
- 1565 Trusel, L. D., Frey, K. E., Das, S. B., Karnauskas, K. B., Munneke, P. K., Van Meijgaard, E. and Van  
Den Broeke, M. R.: Divergent trajectories of Antarctic surface melt under two twenty-first-century  
climate scenarios, *Nature Geoscience*, 8(12), 927, <https://doi.org/10.1038/ngeo2563>, 2015.
- 1570 Turner, J., Hosking, J. S., Phillips, T. and Marshall, G. J.: Temporal and spatial evolution of the  
Antarctic sea ice prior to the September 2012 record maximum extent, *Geophysical Research Letters*,  
40(22), 5894–5898, doi:10.1002/2013GL058371, 2013b.
- 1575 Turner, J., Comiso, J. C., Marshall, G. J., Lachlan-Cope, T. A., Bracegirdle, T., Maksym, T., Meredith,  
M. P., Wang, Z. and Orr, A.: Non-annular atmospheric circulation change induced by stratospheric  
ozone depletion and its role in the recent increase of Antarctic sea ice extent, *Geophysical Research  
Letters*, 36(8), doi: <https://doi.org/10.1029/2009gl037524>, 2009.
- 1580 Turner, J., Phillips, T., Hosking, J. S., Marshall, G. J. and Orr, A.: The Amundsen Sea low, *International  
Journal of Climatology*, 33(7), 1818–1829, doi:<https://doi.org/10.1002/2Fjoc.3558>, 2013a.
- Turner, J., Hosking, J. S., Phillips, T. and Marshall, G. J.: Temporal and spatial evolution of the  
Antarctic sea ice prior to the September 2012 record maximum extent, *Geophysical Research Letters*,  
40(22), 5894–5898, doi:10.1002/2013GL058371, 2013b.
- 1585 Turner, J., Orr, A., Gudmundsson, G. H., Jenkins, A., Bingham, R. G., Hillenbrand, C.-D. and  
Bracegirdle, T. J.: Atmosphere-Ocean-Ice Interactions in the Amundsen Sea Embayment, West  
Antarctica, *Reviews of Geophysics*, doi:<https://doi.org/10.1002/2016rg000532> 2017.
- 1590 Vaughan, D. G., Marshall, G. J., Connolley, W. M., Parkinson, C., Mulvaney, R., Hodgson, D. A.,  
King, J. C., Pudsey, C. J. and Turner, J.: Recent Rapid Regional Climate Warming on the Antarctic  
Peninsula, *Climatic Change*, 60(3), 243–274, doi:10.1023/A:1026021217991, 2003.
- 1595 Wang, Y., Ding, M., van Wessem, J. M., Schlosser, E., Altnau, S., van den Broeke, M. R., Lenaerts, J.  
T. M., Thomas, E. R., Isaksson, E., Wang, J. and Sun, W.: A Comparison of Antarctic Ice Sheet Surface  
Mass Balance from Atmospheric Climate Models and In Situ Observations, *Journal of Climate*, 29(14),  
5317–5337, doi:10.1175/JCLI-D-15-0642.1, 2016.
- 1600 Weertman, J.: Stability of the junction of an ice sheet and an ice shelf, *Journal of Glaciology*, 13, 3–11,  
doi: <https://doi.org/10.3189/s0022143000023327>, 1974.
- Yuan, X. and Martinson, D. G.: The Antarctic dipole and its predictability, *Geophysical Research  
Letters*, 28(18), 3609–3612, doi:<https://doi.org/10.1029/2001gl012969>, 2001.



Page 15 : [3] Supprimé	Authors	26/09/2019 14:56:00
------------------------	---------	---------------------

▼

Page 15 : [3] Supprimé	Authors	26/09/2019 14:56:00
------------------------	---------	---------------------

▼

Page 15 : [4] Supprimé	Authors	26/09/2019 14:56:00
------------------------	---------	---------------------

▼

Page 15 : [5] Supprimé	Authors	26/09/2019 14:56:00
------------------------	---------	---------------------

▼

Page 15 : [6] Supprimé	Authors	26/09/2019 14:56:00
------------------------	---------	---------------------

Page 15 : [7] Supprimé	Authors	26/09/2019 14:56:00
------------------------	---------	---------------------

Page 20 : [8] Supprimé	Authors	26/09/2019 14:56:00
------------------------	---------	---------------------

Page 25 : [9] Supprimé	Authors	26/09/2019 14:56:00
------------------------	---------	---------------------